Main Protease Inhibitors and Drug Surface Hotspot for the Treatment of COVID-19: Drug Repurposing and Molecular Docking Approach

Mahmudul Hasan[a]†, Md Sorwer Alam Parvez[b]†, Kazi Faizul Azim[c], Abdus Shukur Imran[a], Topu Raihan[d], Airin Gulshan[e], Samuel Muhit[f], Rubaiat Nazneen Akhand[g], Md Bashir Uddin[h*#], Syed Sayeem Uddin Ahmed[i*#]

[a]Department of Pharmaceuticals and Industrial Biotechnology, Sylhet Agricultural University, Sylhet 3100, Bangladesh

[b]Department of Genetic Engineering and Biotechnology, Shahjalal University of Science and Technology, Sylhet-3114

[c]Department of Microbial Biotechnology, Sylhet Agricultural University, Sylhet 3100, Bangladesh

[d]Department of Genetic Engineering and Biotechnology, Shahjalal University of Science and Technology, Sylhet-3114

[e]Faculty of Biotechnology and Genetic Engineering, Sylhet Agricultural University, Sylhet 3100, Bangladesh

[f]School of Health Sciences, Central Michigan University, Mount Pleasant, Michigan 48859, United States

[g]Department of Biochemistry and Chemistry, Sylhet Agricultural University, Sylhet 3100, Bangladesh

[h]Department of Medicine, Sylhet Agricultural University, Sylhet 3100, Bangladesh

[i]Department of Epidemiology and Public Health, Sylhet Agricultural University, Sylhet 3100, Bangladesh

†The first two authors contributed equally to this work

#Equal contribution

***Correspondence**

bashir.vetmed@sau.ac.bd [MB Uddin]

ahmedssu.eph@sau.ac.bd [SSU Ahmed]

Main Protease Inhibitors and Drug Surface Hotspot for the Treatment of COVID-19: Drug Repurposing and Molecular Docking Approach

Abstract

The world is facing an unprecedented global pandemic caused by the novel SARS-CoV-2. In the absence of a specific therapeutic agent to treat COVID-19 patients, the present study aimed to virtually screen out the effective drug candidates from the approved main protease protein (MPP) inhibitors and their derivatives for the treatment of SARS-CoV-2. Here, drug repurposing and molecular docking were employed to screen approved MPP inhibitors and their derivatives. The approved MPP inhibitors against HIV and HCV were prioritized, whilst hydroxychloroquine, favipiravir, remdesivir, and alpha-ketoamide were studied as control. The target drug surface hotspot was also investigated through the molecular docking technique. ADME analysis was conducted to understand the pharmacokinetics and drug-likeness of the screened MPP inhibitors. The result of this study revealed that Paritaprevir (-10.9 kcal/mol), and its analog (CID 131982844)(-16.3 kcal/mol) showed better binding affinity than the approved MPP inhibitor compared in this study including favipiravir, remdesivir, and alpha-ketoamide. A comparative study among the screened putative MPP inhibitors revealed that amino acids T25, T26, H41, M49, L141, N142, G143, C145, H164, M165, E166, D187, R188, and Q189 are at critical positions for becoming the surface hotspot in the MPP of SARS-CoV-2. The study also suggested that paritaprevir and its' analog (CID 131982844), may be effective against SARS-CoV-2 as these molecules had the common drug-surface hotspots on the main protease protein of SARS-CoV-2. Other pharmacokinetic parameters also indicate that paritaprevir and its top analog (CID 131982844) will be either similar or better-repurposed drugs than already approved MPP inhibitors.

Keywords: Main protease protein (MPP) inhibitors, SARS-CoV-2, COVID-19, Drug repurposing and Molecular docking

Introduction

COVID-19 is a rapidly spreading viral infectious disease caused by a beta coronavirus – novel coronavirus SASR-CoV-2. The infection was first notified in China in late December 2019, and within three months, 202 countries, territories and conveyance have been reported with COVID-19 cases within their boundaries [1,2]. The emerging human pathogen is causing acute respiratory tract infection with significant morbidity and case fatality. Severe and critical cases require critical and intensive care facilities. The number of critical and intensive care facilities is getting insufficient in some countries and organized health systems of many countries of Asia, Europe and North America are getting incapacitated. COVID-19 has now become a global public health emergency and been declared a pandemic by the World Health Organization [3].

Many efforts are ongoing around the world for the development of effective prevention and treatment strategies for the COVID-19 outbreak. A preventive vaccine development usually takes a long time and might be of use for next pandemic preparedness. Under the present situation, we immediately need a treatment strategy for reducing the catastrophic effect of the ongoing pandemic. Thus, finding out therapy appropriate for the COVID-19 is of paramount importance. Depending on the target, therapies against SARS-CoV-2 can be divided into two categories, the first one is acting on the human immune system or human cells, and the second one is on coronavirus itself [4,5]. Therapies based on the immune system include blocking the signal pathways of human cells that is angiotensin-converting enzyme 2 (ACE2) receptor protein on the surface of cells required for virus replication. In case of therapies based on the virus, retroviral RNA genome encodes for most three necessary enzymes that essential for virus replication: (i) the viral protease (PR) (ii) the reverse transcriptase (RT) and (iii) the integrase (IN) [6–9] where one of the best characterized, conserved drug targets of coronaviruses is the Main Protease Proteins [10,11]. To inhibit the activity of Main Protease Protein (MPP) would be blocking the viral replication, and it would be nontoxic as human proteases with a similar cleavage specificity have already been reported [12,13]. HIV (Human immunodeficiency virus) and HCV (Hepatitis C virus) are both RNA viruses that synthesize a protease from its genome to cut proteins free from long chains and for making mature proteins [14,15]. Protease inhibitors are those drugs that can

inhibit proteases and reduce levels of HIV and HCV to undetectable. Some of those drugs are now repurposing against the COVID-19, which is also a RNA virus and possesses the main protease [16–19]. Computational drug repurposing study previously showed Lopinavir and Ritonavir, two HIV-1 protease inhibitors were identified to be capable of inhibiting SARS-CoV main protease [20] that is why these the drugs used against HIV protease could be used as a homologous target – as the previous SARS-CoV main protease has 96.1% of similarity with the SARS-CoV -2main protease [20]. In the United States, four HCV protease inhibitors have also been recognized for the use in combination with other specified anti-HCV agents, which also suggest the utilization of similar drugs for treatment against the SARS-CoV-2 [21–23].

The observed impact of COVID-19 is differing among countries. However, the number of global diagnosed cases have been exceeded over 1.8 million with a death toll above 1.10 million as of April 12, 2020 [24]. Every day, the number of new cases is increasing exponentially, and expectedly the number of deaths will increase proportionally. Current trend warns us about entering a phase beyond the containment of the disease. These circumstances are pushing the global scientific community high to find out a suitable drug that can be used for the treatment of COVID-19 patients. The discovery of a new drug is a lengthy process. Thus, there is an urgency for repurposing or reprofiling of drugs. Being able to repurpose or reprofile molecules, either already been approved or tested for human safety, would cut down a significant amount of time than the drug discovery process. Identifying existing molecules suitable for the treatment of COVID-19 will lead to immediate clinical trials and subsequent treatment for the patients.

A virtual screening method for finding potential molecules as a drug candidate for particular diseases or pathogens is reliable, time-saving, and cost-effective [25]. Thus, virtual screening method is widely in practice throughout pharmaceutical industries. The molecular docking approach of Computational biology is a powerful tool for screening out the effective drug candidates and has a wide variety of applications in drug discovery and repurposing. Thus, it could be used for repurposing molecules for the treatment of COVID-19. Besides, Computational biology could assist in the field of structural biology, lead molecule optimization, screening out the potential drug candidates, studying the drug surface binding pattern, providing hypothesis to x-ray crystallography to study the substrates and inhibitors, the establishment of a combinatorial library and so on design [26,27].

Repurposing approved drugs against the COVID-2019 epidemic has several advantages, which can help to identify treatment options rapidly [28]. However, three months into the COVID-19 pandemic, but as of now, it is not quite clear about antiviral drugs that could combat the SARS-CoV-2 virus. Worldwide, scientists are racing to find out effective drugs by continuing many studies. Developing a novel drug within a short time against an emerging infectious disease is a time-bound challenge. So, it would be better to rely on a method of repurposing of existing drugs against COVID-19. Here, the current study focuses on the screening of existing main protease inhibitors and their derivatives, including the study of drug-surface hotspots of SARS-CoV-2, by using drug repurposing and computational approaches.

Materials and Methods

Retrieval of main protease proteins (MPP) and MPP inhibitors

The Main Protease Proteins (MPP) structure of SARS-Cov-2 (PDB ID: 6LU7 and PDB ID: 6Y2E) and HCV (PDB ID: 2P59) were retrieved from the genomic information of NCBI and RCSB Protein Data Bank [29,30]. Moreover, the approved MPP inhibitors against HIV and HCV were prioritized for the study. The PDB format for the approved Main Protease Protein (MPP) inhibitors was retrieved from the DrugBank database of NCBI (Supplementary Table 1). Furthermore, the derivatives molecules of topmost screened MPP inhibitors were collected from the NCBI PubChem database (Supplementary Table 2). Moreover, hydroxychloroquine (DrugBank ID: DB01611), favipiravir (DrugBank ID: DB12466), remdesivir (DrugBank ID: DB14761) and alpha-ketoamide (DrugBank ID: CID 6482451) were also retrieved from the NCBI DrugBank database.

Screening of MPP inhibitors against the MPP of SARS-CoV-2

AutoDock Vina software was used for molecular docking experiments, which is now being widely used for screening out the effective therapeutics against the specific drug target of deadly pathogens [30–32]. Prior to molecular docking, the crystal structure of MPP retrieved from protein data bank (PDB ID: 6LU7) was cleaned up by using PyMOL [33] as it was in a complex structure

with an inhibitor. After the removal of unwanted molecules such as water, ions, and inhibitor from the MPP of SARS-CoV-2, it was exposed to 16 approved MPP inhibitors for analyzing the lowest binding energy and interactive amino acids. Moreover, 100 derivatives of top MPP inhibitor candidates found from the initial docking experiment were also exposed to the MPP of SARS-CoV-2 to find out the top one for the treatment of COVID-19. Moreover, Paritaprevir and its top derivatives (CID 131982844) were also exposed to molecular docking with the MPP of HCV (ID: 2P59) and another MPP of SARS-CoV-2 (PDB ID: 6Y2E) suggested by Linlin Zhang et al. 2020 [27]. The grid box parameters were set to a size of 60 A° × 70 A° × 62 A° (x × y × z) and center of -26.289 A° × 13.666 A° × 58.965 A° (x × y × z). Furthermore, another newly released crystal structure of SARS-CoV-2 MPP (PDB ID: 6Y2E) was also used to double check the docking results with the experimental data. The grid box parameters were set to a size of 45 A° × 66 A° × 62 A° (x × y × z) and center of -16.520 A° × -26.112 A° × 17.524 A° (x × y × z) for 'PDB ID: 6Y2E'. LigPlot+ was used to generate the 2D ligand-protein interaction diagrams and to find out the involved amino acids with their interactive position in the docked molecules [34]. Discovery Studio and PyMOL were used to visualize and analyze the ligand molecule interactions with the viral proteins [33,35].

Structural insights of drug surface hotspot in the MPP of SARS-CoV-2

To determine the drug surface hotspot of SARS-CoV-2 main proteasese protein, the docked structures of MPP with the topmost MPP inhibitors were analyzed by LigPlot+, Discovery Studio and PyMOL. The alpha-ketoamide inhibitor, recently suggested by a Linlin Zhang research group for the treatment of COVID-19, was taken as the positive control [36,37]. The molecular docking approach was employed for the study of the binding pattern of α-ketoamide, hydroxychloroquine, favipiravir and remdesivir with the MPP of SARS-CoV-2, and the results enabled a comparative structural analysis of screened MPP inhibitors and their derivatives.

ADME Analysis of Top Drug Candidates

To assess the absorption, distribution, metabolism, and excretion (ADME) properties of the topmost candidates for the MPP inhibitors the Swiss ADME portal was used.

[38]. The Swiss ADME portal is an online platform that is being used successfully to evaluate the pharmacokinetics, drug-likeness, and medicinal chemistry friendliness of possible drug candidates [39]. The study checked out the physico-chemical parameters (formula molecular weight, molar refractivity, TPSA), lipophilicity (Log Po/w (iLOGP), Log Po/w (XLOGP3), Log Po/w (WLOGP), Log Po/w (MLOGP), Log Po/w, (SILICOS-IT), Consensus Log Po/w), and water solubility (Log S: SILICOS-IT, solubility) of the screened topmost MPP inhibitors and their derivatives. To study the drug interaction with the cytochromes P450 (CYP) is one of the crucial in drug discovery that is why the screened MPP inhibitors were employed to study the inhibition effect of different CYP isoforms (CYP1A2 inhibitor, CYP2C19 inhibitor, CYP2C9 inhibitor, CYP2D6 inhibitor, CYP3A4 inhibitor). However, other relevant pharmacokinetic parameters, such as gastrointestinal (GI) absorption, BBB (blood-brain barrier) permeant, and P-gp substrate, were also investigated for putative drug candidate of main protease proteins.

Results

Screening of MPP inhibitors against the MPP of SARS-CoV-2

All of the retrieved PDB structures of approved MPP inhibitors were prepared and optimized for allowing the molecular docking experiment (Supplementary Table 1). Widely used common MPP inhibitors of HCV and HIV (https://www.drugs.com/drug-class/protease-inhibitors.html) were prioritized in the study [40]. There were seven HIV MPP inhibitors (amprenavir, ritonavir, nelfinavir, indinavir, darunavir, fosamprenavir, saquinavir) and six HCV inhibitors (paritaprevir, grazoprevir, glecaprevir, simeprevir, telaprevir, boceprevir) including ssunaprevir, atazanavir, and lopinavir. All of these MPP inhibitors were employed for molecular docking, and the scoring function of AutoDock Vina was utilized to predict the interaction between the above mentioned ligands and the MPP of SARS-CoV-2 (PDB ID: 6LU7). The paritaprevir, an HCV MPP inhibitor, was found to have the highest negative binding energy (-10.9 kcal/mol) when interacting with the MPP of SARS-CoV-2 (Table 1A and Figure 1]. Moreover, glecaprevir (-9.3 kcal/mol), nelfinavir (-8.7 kcal/mol), simeprevir (-8.6 kcal/mol), lopinavir (-8.4 kcal/mol) were also found to be the topmost MPP inhibitors with a high binding affinity (Table 1A). The molecular docking result of all retrieved MPP inhibitors against the MPP of SARS-CoV-2 are listed in Supplementary Table

3. Furthermore, the derivatives of Paritaprevir were allowed to similar molecular docking studies. The top derivative of Paritaprevir "(3S,9Z,12R,15S,17R)-N-cyclopropylsulfonyl-12-methyl-3-[(5-methylpyrazine-2-carbonyl)amino]-2,14-dioxo-17 phenanthridin-6-yloxy-1,13-diazabicyclo[13.3.0]octadec-9-ene-12-carboxamide" (CID 131982844) demonstrated highest binding interaction (-16.3 kcal/mol) with the MPP of SARS-CoV-2 which was better than Paritaprevir (Table 1B, Figure 2 and Figure 3). Approximately 98% of the structural analogs of paritaprevir interacting with the MPP of SARS-CoV-2 showed a higher negative binding energy (>-10 kcal/mol) than that of paritaprevir interacting with the MPP of SARS-CoV-2 (Supplementary Table 4) Moreover, paritaprevir and its top derivatives (CID 131982844) were also exposed to molecular docking with the MPP of HCV (ID: 2P59) and another MPP of SARS-CoV-2 (PDB ID: 6Y2E). The results are given in Table 2. It was found that paritaprevir showed a similar binding pattern as that of the MPP of HCV (-8.4 kcal/mol) and the MPP of SARS-CoV-2 (PDB ID: 6Y2E, -8.4 kcal/mol), as indicated by the previous molecular binding results found for the paritaprevir interaction with the MPP of SARS-CoV-2 (PDB ID: 6LU7). Similar results were also observed in the case of CID 131982844 interactions with the MPP of HCV (-8.4 kcal/mol) and MPP of SARS-CoV-2 (PDB ID: 6Y2E and -8.4 kcal/mol). In addition, alpha-ketoamide (CID 6482451), which has been suggested as an MPP inhibitor based on laboratory experiments, was also exposed to the MPP of SARS-CoV-2 (PDB ID: 6Y2E) as a positive control. The results showed that the binding energy and interaction pattern of alpha-ketoamide (-8.4 kcal/mol) with the MPP of SARS-CoV-2 (Figure 3) was similar to those of paritaprevir and its top derivatives (CID 131982844). In addition, hydroxychloroquine (DB01611), favipiravir (DB12466), and remdesivir (ID: DB14761) were employed for docking analysis of the MPP of SARS-CoV-2. Remdesivir showed the highest negative binding energy (-7.4 kcal/mol) compared to that of hydroxychloroquine (-5.0 kcal/mol) and favipiravir (-4.7 kcal/mol), but these values were lower than those of the MMP inhibitors (paritaprevir (-10.9 kcal/mol) and its derivative (-16.3 kcal/mol) found in the present study (Table 2 and Figure 4).

Structural insights of drug surface hotspot in the MPP of SARS-CoV-2

To determine the common interactive sites of MPP in SARS-CoV-2, the molecular docking pattern and involved amino acid residues with their respective position were analyzed. The molecular

docking study results of MPP inhibitors, derivatives and the control group with the MPP of SARS-CoV-2 and HCV were closely investigated to determine the common drug-surface hotspots.. From the molecular docking study, the five approved MPP inhibitors (paritaprevir, glecaprevir, nelfinavir, simeprevir and lopinavir) were screened for the best ligand molecules bound with the MPP of SARS-CoV-2 (Supplementary Table 1). As with the general screen, the derivatives of paritaprevir were also screened, and the 10 topmost paritaprevir derivative interaction patterns were also analyzed to understand the common drug-surface hotspots on the MPP of SARS-CoV-2 (Table 1B). Here, Paritaprevir was found to be involved with the amino acid of R131, K137, T169, A194, T196, D197, K236, Y237, N238, L286, L287 and D289 in the MPP (PDB ID 6LU7) of SARS-CoV-2 (Figure 1). The position of N238, L286, and L287 were also crucial for the binding of MPP inhibitors simeprevir (K5, Q12, K137, T199, N238, L272, L286, L287, D289) and glecaprevir (T199, K236, Y237, L271, G275, M276, N277, G278, L286, L287) (Table 1A). Most relevant results of binding with MPP were found in the case of nelfinavir. There were 13 amino acid positions (T25, T26, H41, M49, F140, L141, N142, H163, H164, E166, D187, R188, Q189) in the docking site of nelfinavir which positions were also abundantly found in the most of paritaprevir derivatives (Figure 2). Moreover, alpha-ketoamide inhibitors, reported for the inhibition of MPP by lab experiment, was also employed for the interaction study with the MPP (PDB ID: 6LU7) of SARS-CoV-2 (Figure 3). Most surprisingly, amino acids, such as T25, L27, H41, M49, F140, N142, C145, H163, H164, pl M165, E166, H172, R188 and Q189, were found to have critical positions in the alpha-ketoamide inhibitor interactions with MPP, and these amino acids were also found in nelfinavir and derivatives of paritaprevir. Again, another MPP structure (PDB ID: 6Y2E), reported for alpha-ketoamide inhibitors were also docked with the topmost MPP inhibitors found from the present study, and the lopinavir were found the similar binding pattern with both structures of MPP of SARS-CoV-2 what found from paritaprevir (Table 1B and Table 2). Besides, Binding pattern of remdesivir (T25, T26, H41, M49, L141, N142, G143, C145, H164, M165, E166, D187, R188, Q189) with the MPP of SARS-CoV-2 (Figure 4) was highly similar with the binding interaction of Nelfinavir (T25, T26, H41, M49, F140, L141, N142, H163, H164, E166, D187, R188, Q189), alpha-ketoamide (T25, L27, H41, M49, F140, N142, C145, H163, H164, M165, E166, H172, R188, Q189) and all of the topmost derivatives of paritaprevir (T25, T26, L27, H41, M49, F140, L141, N142, G143, C145, H164, M165, E166, D187, Q189). The binding patterns from MPP inhibitors, derivatives and experimentally suggested molecules

indicates that that T25, T26, H41, M49, L141, N142, G143, C145, H164, M165, E166, D187, R188 and Q189 could be the critical amino acid positions for drug surface hotspot in the MPP of SARS-CoV-2 (Figure 5).

ADME Analysis of Top Drug Candidates

The physico-chemical parameters, lipophilicity, pharmacokinetics properties and water solubility were studied for the topmost putative MPP inhibitors (paritaprevir, glecaprevir, nelfinavir, simeprevir, and lopinavir) and the derivatives of Paritaprevir (Table 3 and Supplementary Table 5). Formula, molecular weight, molar refractivity and TPSA were determained. Lipophilicity, partition coefficient between n-octanol and water (log Po/w) were also calculated by using five commonly freely available predictive models (XLOGP3, WLOGP, MLOGP, SILICOS-IT, iLOGP) [41]. The result of the drug interaction with the cytochrome P450 (CYP) indicates that only paritaprevir had an inhibitory effect on CYP3A4, while glecaprevir had no interaction with the cytochromes P450 (CYP) isoforms. Moreover, cytochrome CYP1A2, CYP2C9 and CYP2D6 had no interaction with the top putative MPP inhibitors. Also, there was no interaction possibility of the top paritaprevir derivatives with the cytochrome CYP1A2, CYP2C19, CYP2C9, and CYP2D6 (Supplementary Table 5). However, GI absorption was found lower in case of paritaprevir, glecaprevir, nelfinavir and simeprevir and the top paritaprevir derivatives. The blood-brain barrier (BBB) permeation was also calculated by BOILED-Egg models [42], and there was no BBB permeant among putative MPP inhibitors and paritaprevir derivatives. The study revealed the water solubility levels of paritaprevir (1.38e-07 mg/ml; 1.81e-10 mol/l), glecaprevir (9.22e-06 mg/ml; 1.10e-08 mol/l), nelfinavir (3.11e-05 mg/ml; 5.48e-08 mol/l), simeprevir (1.21e-06 mg/ml; 1.61e-09 mol/l) and lopinavir (5.57e-08 mg/ml; 8.85e-11 mol/l). In addition, the top ten derivatives of paritaprevir were also subjected to ADME analysis, and the details of the analysis are included in Supplementary Table 5.

Discussion

The newly emerged coronavirus has created a global health crisis. The pandemic has already broken previous records set by other types of coronaviruses, such as SARS and MERS. The present

study aimed to screen and suggest potential drug candidates against SARS-CoV to combat the global pandemic of COVID-19. The study suggested that paritaprevir, glecaprevir, nelfinavir, simeprevir and lopinavir along with their top derivatives may be effective against SARS-CoV-2, and these molecules also had the common drug-surface hotspots on the main protease protein of SARS-CoV-2.

COVID-19 has become a great challenge for international policymakers and scientific communities [43,44]. SARS-CoV-2 virus is spreading around the world, and pandemic attitude has established. The morbidity is increasing, and hospitals are running out of capacity to handle critical cases. However, there is no drug to kill the virus or vaccine to protect it. The present study aimed to screen and suggest potential drug candidates against SARS-CoV to combat the global pandemic of COVID-19. The study suggested that paritaprevir, glecaprevir, nelfinavir, simeprevir and lopinavir along with their top derivatives, may be effective against SARS-CoV-2, and these molecules also had the common drug-surface hotspots on the main protease protein of SARS-CoV-2.

Though there are numerous research and ongoing discussions on the efficacy of different drug candidates – namely, hydroxychloroquine, favipiravir, remdesivir, and alpha-ketoamide [45,46]. Virtual screening for drug repurposing is becoming vital for finding drugs that could be used for the treatment of COVID-19. Thus, we have taken endeavor to screen drugs been approved and indicated for the treatment of other viral diseases. In the present study, the Main Protease Protein(MPP) of HIV and HCV were prioritized to check out the efficacy of MPP inhibitors of SARS-CoV-2, as those MPP inhibitors have already showed effective notions against different viral pathogens [47,48]. Here, drug repurposing with the molecular docking approach was employed for the comprehensive screening and analysis of the putative drug candidates against the SARS-CoV-2. Moreover, to determine the common drug surface hotspot in the MPP of SARS-CoV-2, different recently studied MPP inhibitors of SARS-CoV-2, such as alpha-ketoamide, hydroxychloroquine, remdesivir and favipiravir [49–51] were also investigated with the approved MPP inhibitors and their derivatives.

From the analysis of molecular docking studies, it was found that paritaprevir, glecaprevir, nelfinavir, simeprevir and lopinavir could be potential main protease protein inhibitors of SARS-CoV-2, where lopinavir has been previously reported by different studies for the treatment of COVID-19 [52]. Paritaprevir [53], Glecaprevir [54], Nelfinavir [55], and Simeprevir [56] had already been approved for the treatment of HIV or HCV [57], and the results of this study indicate that those could be the potential drug candidate of SARS-CoV-2 than Lopinavir. Again, the present study also investigated the binding pattern of the screened MPP inhibitors along with few experimentally trailed or suggested drug molecules such as alpha-ketoamide, hydroxychloroquine, favipiravir, and remdesivir with MPP of SARS-CoV-2. Surprisingly, the screened MPP inhibitors had similar, and in some cases, higher binding affinity with the main protease protein of SARS-CoV-2. Approximately 100 derivatives of paritaprevir were also investigated through its molecular docking with SARS-CoV-2, and one of the paritaprevir derivatives "(3S,9Z,12R,15S,17R)-N-cyclopropylsulfonyl-12-methyl-3-[(5-methyl pyrazine-2-carbonyl)amino]-2,14-dioxo-17 phenanthridin-6-yloxy-1,13-diazabicyclo [13.3.0]octadec-9-ene-12-carboxamide (CID 131982844)'' was found to have the highest binding affinity in terms of global energy than already approved MPP inhibitors for the treatment of COVID-19. This paritaprevir derivative (CID 131982844) could be the better-dug candidate for the inhibition of MPP of SARS-CoV-2. The docking algorithm search for potential energy algorithm and rank binding affinity of molecules based on global energy minimum [58].

The study of drug surface hotspot is the pre-requisite for understanding the molecular interaction between drug candidates and target molecules [59,60]. It has been revealed that the molecular binding site of nelfinavir, remdesivir, alpha-kemoamide, and all of the paritaprevir derivatives had a similar pattern that may indicate drug surface hotspot in the MPP of SARS-CoV-2. Some of these positions were also found common in the paritaprevir, glecaprevir, simeprevir, and lopinavir. The investigation suggested that amino acids T25, T26, H41, M49, L141, N142, G143, C145, H164, M165, E166, D187, R188 and Q189 in the MPP could effectively interact with the drug molecules.

Top screened drug candidates from MPP inhibitors and their derivatives were also employed for ADME analysis. Physico-chemical parameters, lipophilicity, pharmacokinetics properties, and

water solubility were studied, which contributes to the analysis of ADME properties. The study of cytochromes P450 (CYP) isoforms inhibition concluded that the suggested MPP inhibitors and paritaprevir derivatives had fewer possibilities to interact with cytochromes P450 (CYP) isoforms. Blood-brain barrier (BBB) permeation and water solubility of putative MPP inhibitors were also calculated. There was no BBB permeant in the screened MPP inhibitors and paritaprevir derivatives.

The results provided in the present study suggest that paritaprevir and its' analog (CID 131982844) could be a promising option for treating SARS-CoV-2, than already approved other MPP inhibitors like favipiravir and remdesivir. The results of this current study are limited to in-silico analysis and lack of *in-vivo* efficacy testing. At present, multiple MPP inhibitors like favipiravir and remdesivir and other drugs are currently under evaluation through randomized control trials. Thus, we strongly suggest a quick assessment of paritaprevir and its' analog (CID 131982844), through a clinical trial, as a potential candidate for the treatment of COVID-19 patients.

Funding

No funding was received for this work.

Author's contributions

Conception and design: SSU Ahmed, MB Uddin, M Hasan, MSA Parvez

Performed the research and data acquisition: M Hasan, MSA Parvez, KFAzim, AS Imran, T Raihan, A Gulshan, S Muhit, RN Akhand

Analysis and interpretations of data: M Hasan, MSA Parvez, KFAzim, AS Imran, T Raihan, A Gulshan, S Muhit, RN Akhand

Manuscript draft, review and editing: M Hasan, MSA Parvez, KFAzim, AS Imran, T Raihan, A Gulshan, S Muhit, RN Akhand, MB Uddin, SSU Ahmed

Study supervision: MB Uddin, SSU Ahmed

All authors read and approved the final version of the manuscript.

Declaration of interests

The authors declare that they have no known competing financial interests or personal relationships that could have appeared to influence the work reported in this paper.

Data availability

All data generated and analysed during this study is included in the main manuscript or supplementary files.

References

[1] Huang C, Wang Y, Li X, Ren L, Zhao J, Hu Y, et al. Clinical features of patients infected with 2019 novel coronavirus in Wuhan, China. Lancet 2020;395:497–506. doi:10.1016/S0140-6736(20)30183-5.

[2] Ren L-L, Wang Y-M, Wu Z-Q, Xiang Z-C, Guo L, Xu T, et al. Identification of a novel coronavirus causing severe pneumonia in human. Chin Med J (Engl) 2020:1. doi:10.1097/cm9.0000000000000722.

[3] WHO. (World Health Organization): Coronavirus disease (COVID-2019) situation reports. https://www.who.int/emergencies/diseases/novel-coronavirus-2019/situation-reports/. Retrieved on 4 April, 2020. 2020.

[4] Wu C, Liu Y, Yang Y, Zhang P, Zhong W, Wang Y, et al. Analysis of therapeutic targets for SARS-CoV-2 and discovery of potential drugs by computational methods. Acta Pharm Sin B 2020. doi:10.1016/j.apsb.2020.02.008.

[5] Omrani AS, Saad MM, Baig K, Bahloul A, Abdul-Matin M, Alaidaroos AY, et al. Ribavirin and interferon alfa-2a for severe Middle East respiratory syndrome coronavirus infection: A retrospective cohort study. Lancet Infect Dis 2014;14:1090–5. doi:10.1016/S1473-3099(14)70920-X.

[6] Tözsér J. Comparative studies on retroviral proteases: Substrate specificity. Viruses

2010;2:147–65. doi:10.3390/v2010147.

[7] Zhao J, Li K, Wohlford-Lenane C, Agnihothram SS, Fett C, Zhao J, et al. Rapid generation of a mouse model for Middle East respiratory syndrome. Proc Natl Acad Sci U S A 2014;111:4970–5. doi:10.1073/pnas.1323279111.

[8] Agrawal AS, Garron T, Tao X, Peng B-H, Wakamiya M, Chan T-S, et al. Generation of a Transgenic Mouse Model of Middle East Respiratory Syndrome Coronavirus Infection and Disease. J Virol 2015;89:3659–70. doi:10.1128/jvi.03427-14.

[9] Macchiagodena M, Pagliai M, Procacci P. Inhibition of the Main Protease 3CL-pro of the Coronavirus Disease 19 via Structure-Based Ligand Design and Molecular Modeling. Https://ArxivOrg/Pdf/200209937Pdf 2020:1–28.

[10] García-Fernández R, Ziegelmüller P, González L, Mansur M, Machado Y, Redecke L, et al. Two variants of the major serine protease inhibitor from the sea anemone Stichodactyla helianthus, expressed in Pichia pastoris. Protein Expr Purif 2016;123:42–50. doi:10.1016/j.pep.2016.03.003.

[11] Hilgenfeld R. From SARS to MERS: crystallographic studies on coronaviral proteases enable antiviral drug design. FEBS J 2014;281:4085–96. doi:10.1111/febs.12936.

[12] Zhang L, Lin D, Sun X, Curth U, Drosten C, Sauerhering L, et al. Crystal structure of SARS-CoV-2 main protease provides a basis for design of improved α-ketoamide inhibitors. Science 2020;3405:1–9. doi:10.1126/science.abb3405.

[13] Li G, De Clercq E. Therapeutic options for the 2019 novel coronavirus (2019-nCoV). Nat Rev Drug Discov 2020;19:149–50. doi:10.1038/d41573-020-00016-0.

[14] Banerjee R, Dasgupta A. Specific Interaction of Hepatitis C Virus Protease/Helicase NS3 with the 3'-Terminal Sequences of Viral Positive- and Negative-Strand RNA. J Virol 2001;75:1708–21. doi:10.1128/jvi.75.4.1708-1721.2001.

[15] Zhou Y, Hou Y, Shen J, Huang Y, Martin W, Cheng F. Network-based drug repurposing for novel coronavirus 2019-nCoV/SARS-CoV-2. Cell Discov 2020;6. doi:10.1038/s41421-020-0153-3.

[16] Lu H. Drug treatment options for the 2019-new coronavirus (2019-nCoV). Biosci Trends 2020;14:69–71. doi:10.1002/jmv.25678.4.

[17] Sacks FM, Harris A, Sc M, Johnson DW, Ph D, Kesselhut J, et al. Class-sparing regimens for initial treatment of HIV-1 infection. N Engl J Med 2008;358:2095-2106. doi:10.1056/NEJMoa1109071.

[18] Dayer MR. Old Drugs for Newly Emerging Viral Disease, COVID-19: Bioinformatic Prospective. Https://ArxivOrg/Ftp/Arxiv/Papers/2003/200304524Pdf 2020.

[19] Salazar J, Courter J, Girotto J. Role of tipranavir in treatment of patients with multidrug-resistant HIV. Ther Clin Risk Manag 2010;Volume 6:431–41. doi:10.2147/tcrm.s4207.

[20] Nukoolkarn V, Lee VS, Malaisree M, Aruksakulwong O, Hannongbua S. Potential Inhibitor of COVID-19 Main Protease (Mpro) From Several Medicinal Plant Compounds by Molecular Docking Study. J Theor Biol 2008;254:861–7. doi:10.1016/j.jtbi.2008.07.030.

[21] Ann D. Kwong RBPSG. Development and Marketing of INCIVEK (Telaprevir; VX-950): A First-Generation HCV Protease Inhibitor, in Combination with PEGylated Interferon and Ribavirin. Top Med Chem 2014;9:1–68. doi:10.1007/7355.

[22] de Leuw P, Stephan C. Protease inhibitors for the treatment of hepatitis C virus infection. GMS Infect Dis 2017;5:Doc08. doi:10.3205/id000034.

[23] Ezat AA, Elfiky AA, Elshemey WM, Saleh NA. Novel inhibitors against wild-type and mutated HCV NS3 serine protease: an in silico study. VirusDisease 2019;30:207–13. doi:10.1007/s13337-019-00516-7.

[24] Worldometers. COVID-19 Coronavirus outbreak. 2020. https://www.worldometers.info/coronavirus/. Retrieved 12 April 2020. 2020.

[25] Anh Vu L, Thi Cam Quyen P, Thuy Huong N. In silico Drug Design: Prospective for Drug Lead Discovery. Int J Eng Sci Invent 2015;4:60–70.

[26] Meng XY, Zhang HX, Mezei M CM. Molecular Docking: A powerful approach for structure-baseddrug discovery. Bone 2008;23:1–7. doi:10.1038/jid.2014.371.

[27] Brogi S. Computational approaches for drug discovery. Molecules 2019;24:1–6. doi:10.3390/molecules24173061.

[28] Li X, Yu J, Zhang Z, Ren J, Peluffo AE, Zhang W, et al. Network Bioinformatics Analysis Provides Insight into Drug Repurposing for COVID-2019. Https://WwwPreprintsOrg/Manuscript/2020030286/V1 2020. doi:10.20944/PREPRINTS202003.0286.V1.

[29] Agarwala R, Barrett T, Beck J, Benson DA, Bollin C, Bolton E, et al. Database resources of the National Center for Biotechnology Information. Nucleic Acids Res 2016;44:D7–19. doi:10.1093/nar/gkv1290.

[30] Rose PW, Prlić A, Altunkaya A, Bi C, Bradley AR, Christie CH, et al. The RCSB protein data bank: Integrative view of protein, gene and 3D structural information. Nucleic Acids Res 2017;45:D271–81. doi:10.1093/nar/gkw1000.

[31] Waterhouse AM, Procter JB, Martin DMA, Clamp M, Barton GJ. Jalview Version 2-A multiple sequence alignment editor and analysis workbench. Bioinformatics 2009;25:1189–91. doi:10.1093/bioinformatics/btp033.

[32] Anil KTJW. Autodock vina: improving the speed and accuracy of docking. J Comput Chem 2019;31:455–61. doi:10.1002/jcc.21334.AutoDock.

[33] L DeLano W. Pymol: An open-source molecular graphics tool. Newsl Protein Crystallogr 2002;40.

[34] RA L, MB S. LigPlot+: multiple ligand-protein interaction diagrams for drug discovery. J Chem Inf Model 2011;51:2778–86.

[35] Wang Q, He J, Wu D, Wang J, Yan J, Li H. Interaction of α-cyperone with human serum albumin: Determination of the binding site by using Discovery Studio and via spectroscopic methods. J Lumin 2015;164:81–5. doi:10.1016/j.jlumin.2015.03.025.

[36] Zhang L, Lin D, Kusov Y, Nian Y, Ma Q, Wang J, et al. α-Ketoamides as Broad-Spectrum Inhibitors of Coronavirus and Enterovirus Replication: Structure-Based Design, Synthesis, and Activity Assessment. J Med Chem 2020. doi:10.1021/acs.jmedchem.9b01828.

[37] Zhang L, Lin D, Sun X, Rox K, Hilgenfeld R. X-ray Structure of Main Protease of the Novel Coronavirus SARS-CoV-2 Enables Design of α-Ketoamide Inhibitors. BioRxiv 2020:2020.02.17.952879. doi:10.1101/2020.02.17.952879.

[38] Daina A, Michielin O, Zoete V. SwissADME: A free web tool to evaluate pharmacokinetics, drug-likeness and medicinal chemistry friendliness of small molecules. Sci Rep 2017;7:1–13. doi:10.1038/srep42717.

[39] Tripathi P, Ghosh S, Talapatra SN. Bioavailability prediction of phytochemicals present in Calotropis procera (Aiton) R . Br . by using Swiss-ADME tool 2019;131:147–63.

[40] Agbowuro AA, Huston WM, Gamble AB, Tyndall JDA. Proteases and protease inhibitors in infectious diseases. Med Res Rev 2018;38:1295–331. doi:10.1002/med.21475.

[41] Arnott JA, Planey SL. The influence of lipophilicity in drug discovery and design. Expert Opin Drug Discov 2012;7:863–75. doi:10.1517/17460441.2012.714363.

[42] Daina A, Zoete V. A BOILED-Egg To Predict Gastrointestinal Absorption and Brain Penetration of Small Molecules. ChemMedChem 2016:1117–21. doi:10.1002/cmdc.201600182.

[43] Wilder-Smith A, Chiew CJ, Lee VJ. Can we contain the COVID-19 outbreak with the same measures as for SARS? Lancet Infect Dis 2020;3099. doi:10.1016/S1473-3099(20)30129-8.

[44] Yuen K-S, Ye Z-W, Fung S-Y, Chan C-P, Jin D-Y. SARS-CoV-2 and COVID-19: The most important research questions. Cell Biosci 2020;10:40. doi:10.1186/s13578-020-00404-4.

[45] Dong L, Hu S, Gao J. Discovering drugs to treat coronavirus disease 2019 (COVID-19). Drug Discov Ther 2020;14:58–60. doi:10.5582/ddt.2020.01012.

[46] Zhou D, Dai SM TQ. COVID-19: a recommendation to examine the effect of hydroxychloroquine in preventing infection and progression. J Antimicrob Chemother 2020:4–7. doi:10.1093/jac/dkaa114.

[47] Asselah T, Kowdley K V., Zadeikis N, Wang S, Hassanein T, Horsmans Y, et al. Efficacy

of Glecaprevir/Pibrentasvir for 8 or 12 Weeks in Patients With Hepatitis C Virus Genotype 2, 4, 5, or 6 Infection Without Cirrhosis. Clin Gastroenterol Hepatol 2018;16:417–26. doi:10.1016/j.cgh.2017.09.027.

[48] Reau N, Kwo PY, Rhee S, Brown RS, Agarwal K, Angus P, et al. Glecaprevir/Pibrentasvir Treatment in Liver or Kidney Transplant Patients With Hepatitis C Virus Infection. Hepatology 2018;68:1298–307. doi:10.1002/hep.30046.

[49] Al-Tawfiq JA, Al-Homoud AH, Memish ZA. Remdesivir as a possible therapeutic option for the COVID-19. Travel Med Infect Dis 2020:101615. doi:10.1016/j.tmaid.2020.101615.

[50] Colson P, Rolain J-M, Lagier J-C, Brouqui P, Raoult D. Chloroquine and hydroxychloroquine as available weapons to fight COVID-19. Int J Antimicrob Agents 2020:105932. doi:10.1016/j.ijantimicag.2020.105932.

[51] Chen C, Huang J, Cheng Z, Wu J, Chen S, Zhang Y, et al. Favipiravir versus Arbidol for COVID-19: A Randomized Clinical Trial. MedRxiv 2020:2020.03.17.20037432. doi:10.1101/2020.03.17.20037432.

[52] Cao B, Wang Y, Wen D, Liu W, Wang J, Fan G, et al. A Trial of Lopinavir-Ritonavir in Adults Hospitalized with Severe Covid-19. N Engl J Med 2020:1–13. doi:10.1056/NEJMoa2001282.

[53] Sulkowski MS, Eron OJ, Wyles D, Trinh R, Lalezari J, Wang C, et al. Ombitasvir, Paritaprevir Co-dosed with Ritonavir, Dasabuvir, and Ribavirin for Hepatitis C in Patients Co-infected with HIV-1 a Randomized Trial. JAMA - J Am Med Assoc 2015;313:1223–31. doi:10.1001/jama.2015.1328.

[54] Gane E, Lawitz E, Pugatch D, Papatheodoridis G, Bräu N, Brown A, et al. Glecaprevir and pibrentasvir in patients with HCV and severe renal impairment. N Engl J Med 2017;377:1448–55. doi:10.1056/NEJMoa1704053.

[55] Regazzi M, Maserati R, Villani P, Cusato M, Zucchi P, Briganti E, et al. Clinical pharmacokinetics of nelfinavir and its metabolite M8 in human immunodeficiency virus (HIV)-positive and HIV-hepatitis C virus-coinfected subjects. Antimicrob Agents

Chemother 2005;49:643–9. doi:10.1128/AAC.49.2.643-649.2005.

[56] Dieterich D, Rockstroh JK, Orkin C, Gutiérrez F, Klein MB, Reynes J, et al. Simeprevir (TMC435) with pegylated interferon/ribavirin in patients coinfected with HCV Genotype 1 and HIV-1: A Phase 3 study. Clin Infect Dis 2014;59:1579–87. doi:10.1093/cid/ciu675.

[57] Kumar RN, Balba GP. Managing the HIV/HCV-Co-Infected Patient in the Direct-Acting Antiviral Era: a Review of Pertinent Drug Interactions. Curr Treat Options Infect Dis 2017;9:411–24. doi:10.1007/s40506-017-0138-4.

[58] Brooijmans N, Kuntz ID. Molecular recognition and docking algorithms. Annu Rev Biophys Biomol Struct 2003;32:335–73. doi:10.1146/annurev.biophys.32.110601.142532.

[59] Rosell M, Fernández-Recio J. Hot-spot analysis for drug discovery targeting protein-protein interactions. Expert Opin Drug Discov 2018;13:327–38. doi:10.1080/17460441.2018.1430763.

[60] Lionta E, Spyrou G, Vassilatis D, Cournia Z. Structure-Based Virtual Screening for Drug Discovery: Principles, Applications and Recent Advances. Curr Top Med Chem 2014;14:1923–38. doi:10.2174/1568026614666140929124445.

Figures

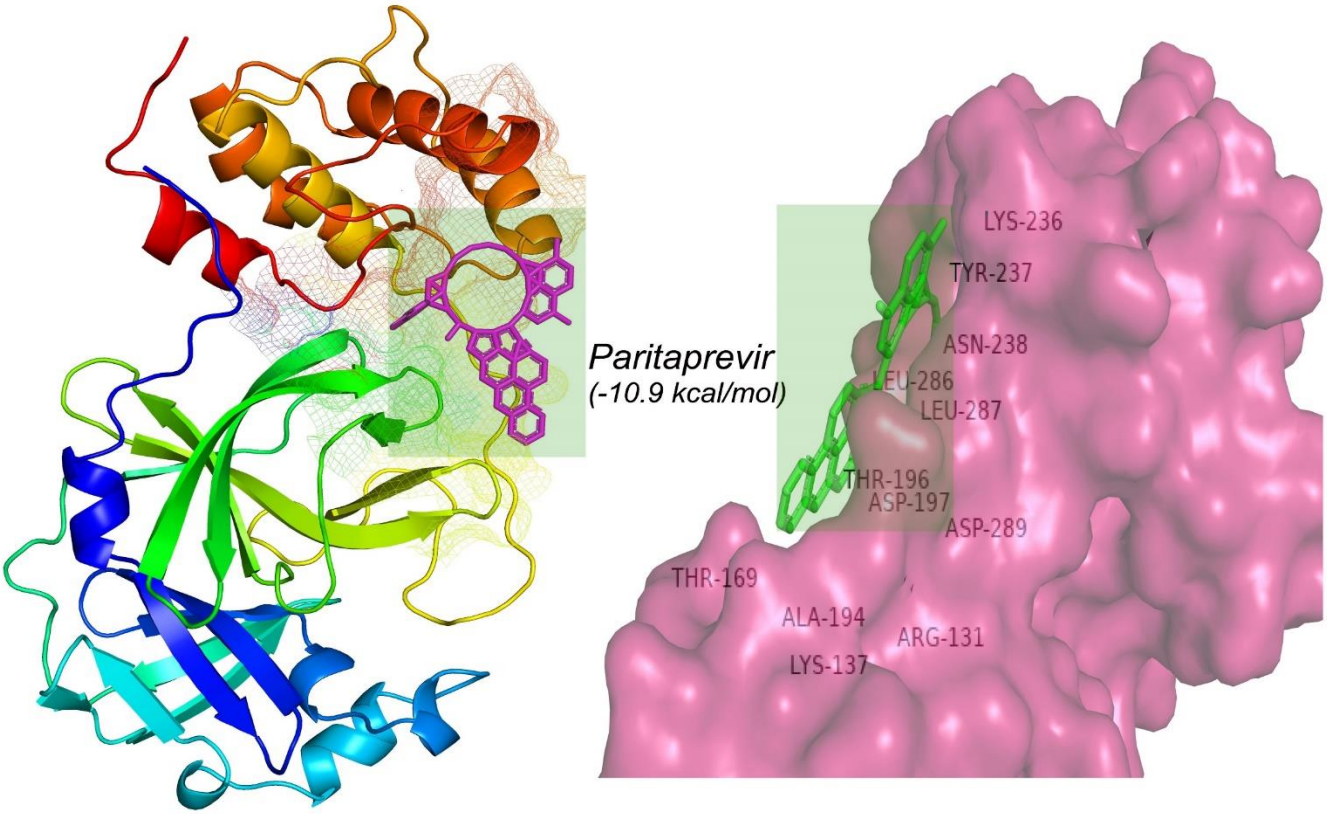

Figure 1: Molecular interaction between Paritaprevir and Main Protease Protein of SARS-CoV-2.

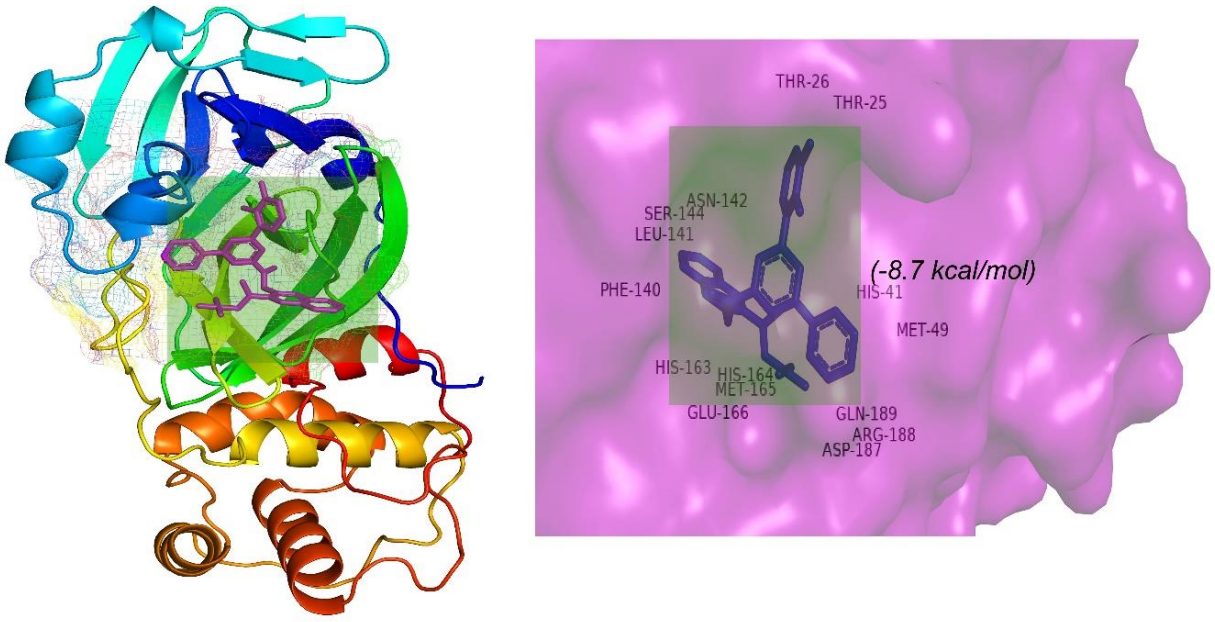

(A) Nelfinavir

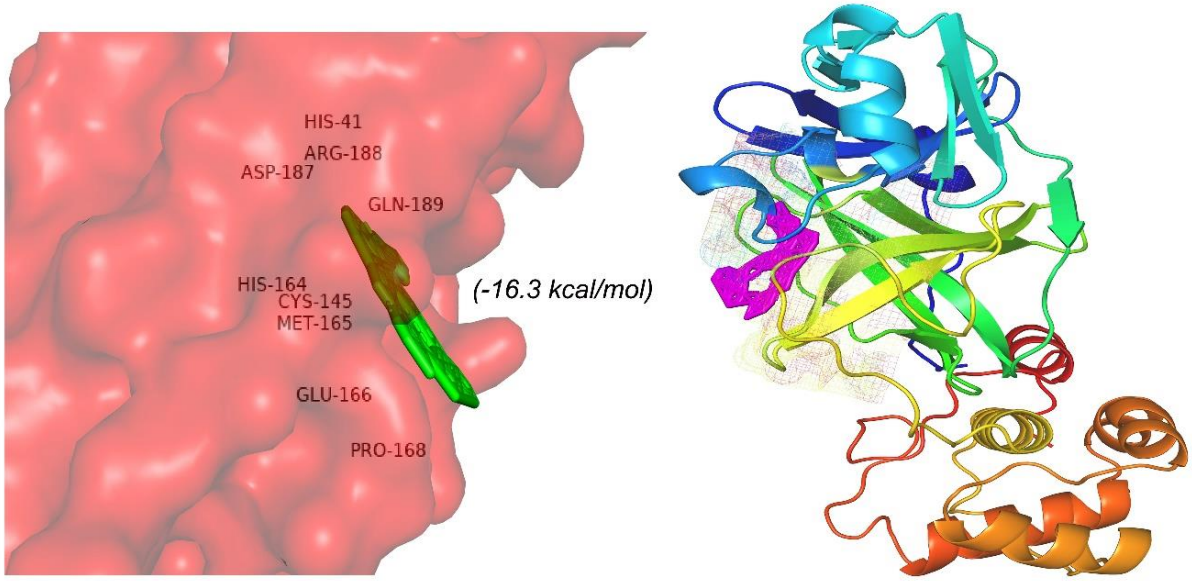

(B) Top Paritaprevir Derivative (CID 131982844)

Figure 2: Molecular insights of Main Protease Protein interactions with (A) Nelfinavir and top (B) Paritaprevir derivative.

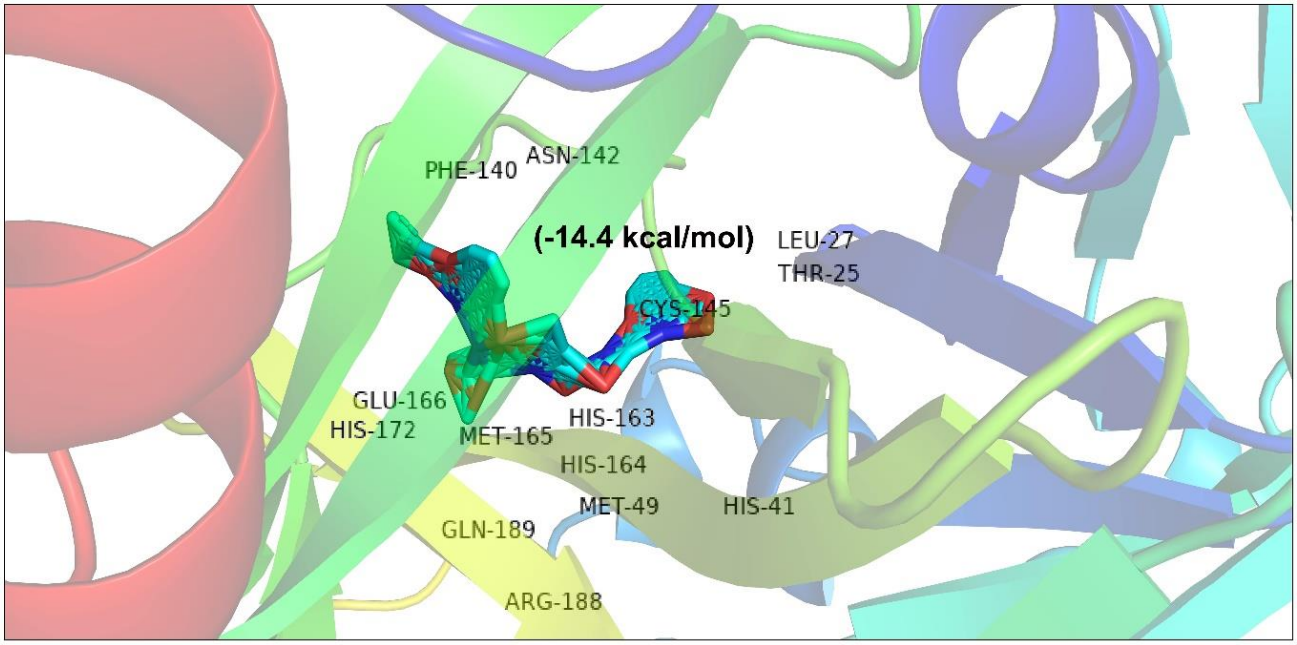

(A) Alpha-Ketoamide

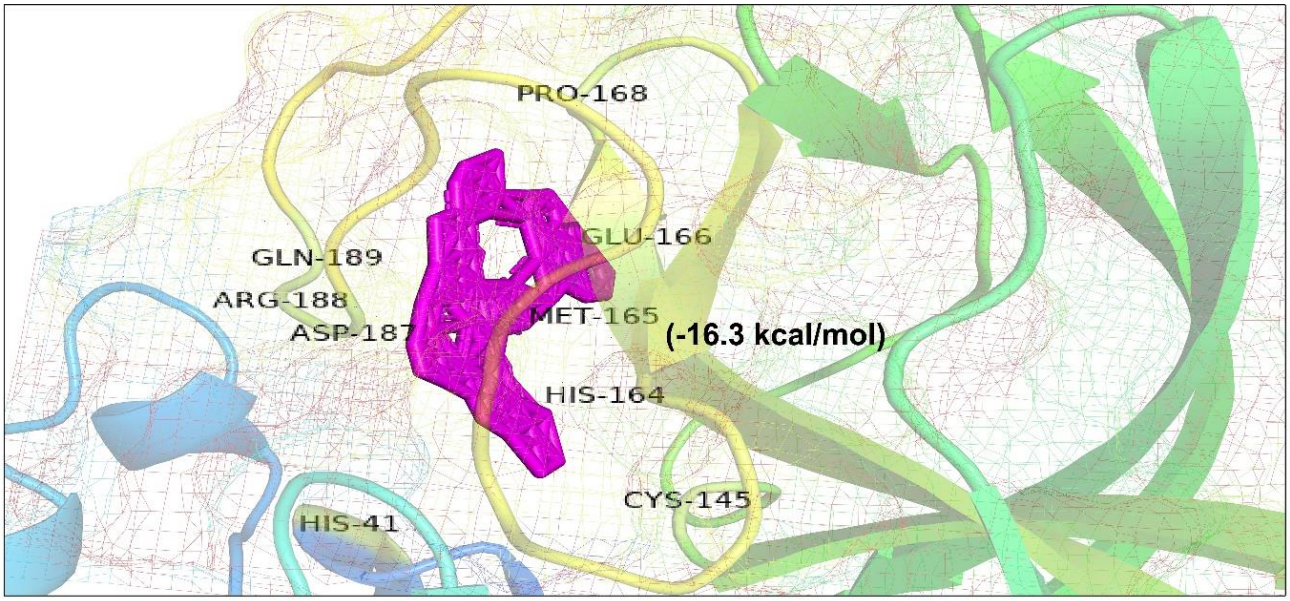

(B) Top Paritaprevir Derivative (CID 131982844)

Figure 3: Structural overview of molecular interaction of (A) Alpha-ketoamide and top (B) Paritaprevir derivative with Main Protease Protein of SARS-CoV-2.

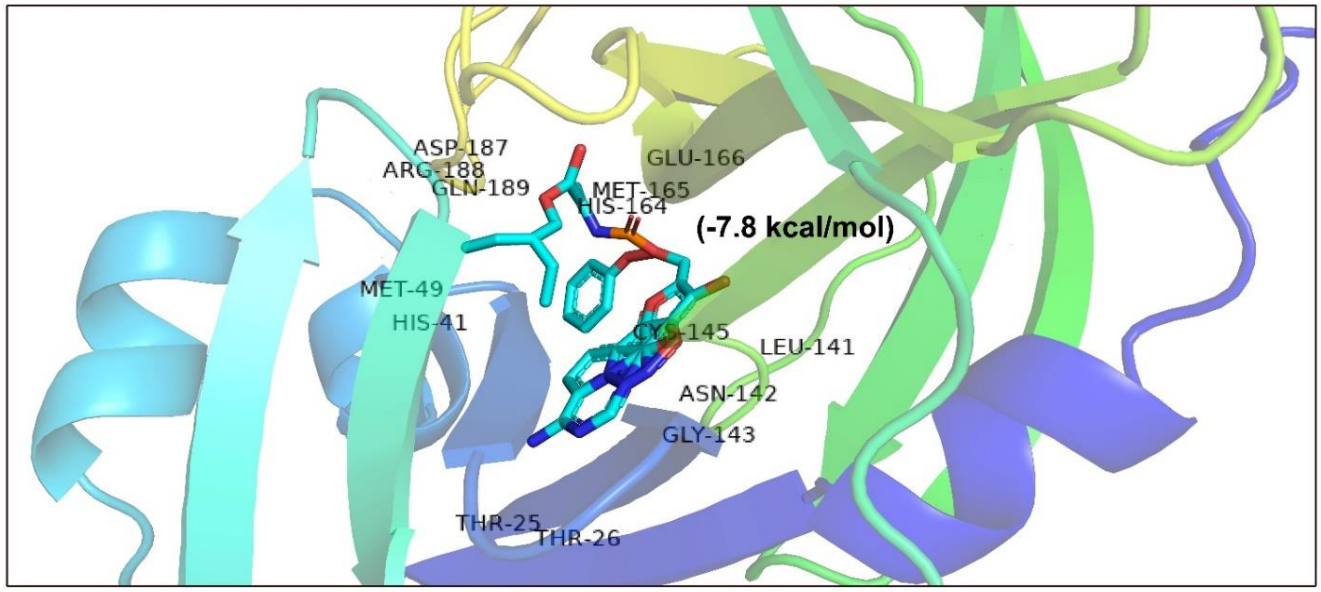

(A) Remdesivir

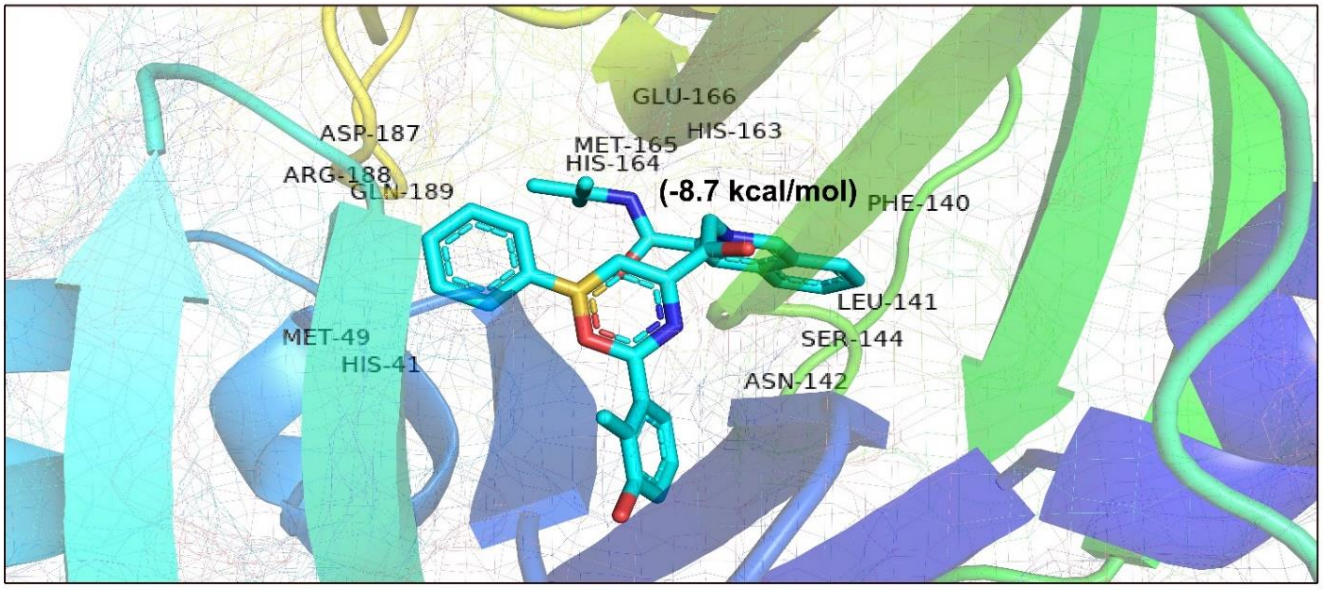

(B) Nelfinavir

Figure 4: Drug surface overview from the interaction of (A) Remdesivir and (B) Nelfinavir with Main Protease Protein of SARS-CoV-2.

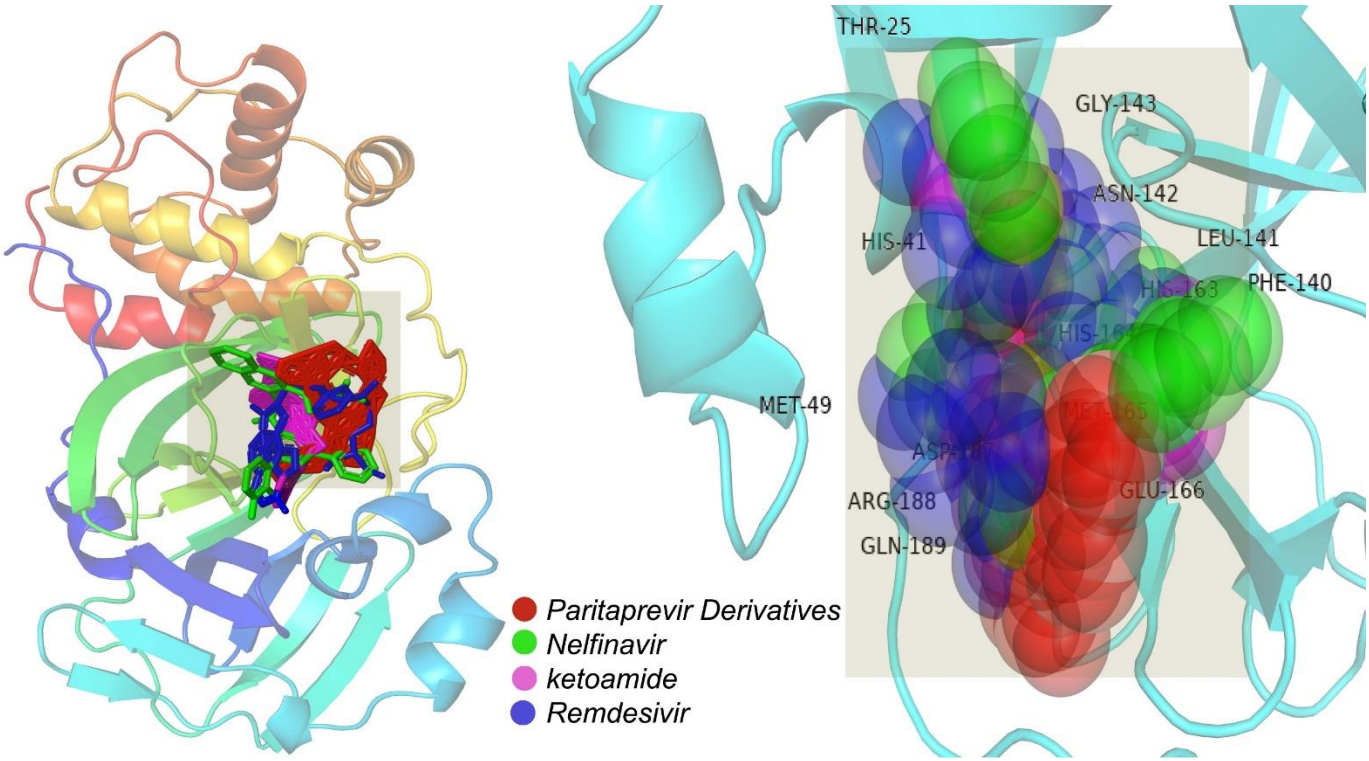

Figure 5: Structural insights of common surface of drug hotspot in the Main Protease Protein of SARS-CoV-2.

Table 1 (A): Molecular docking results of top five MPP inhibitors including interactive amino acids from SARS-CoV-2 MPP.

Drug Name	***Binding Energy (kcal/mol)***	***Involved Amino Acid with Position***
Paritaprevir	-10.9	R131, K137, T169, A194, T196, D197, K236, Y237, N238, L286, L287, D289
Glecaprevir	-9.3	T199, K236, Y237, L271, G275, M276, N277, G278, L286, L287
Nelfinavir	-8.7	T25, T26, H41, M49, F140, L141, N142, S144, H163, H164, M165, E166, D187, R188, Q189
Simeprevir	-8.6	K5, Q12, K137, T199, N238, L272, L286, L287, D289
Lopinavir	-8.4	Q107, Q110, V202, E240, P241, T243, H246, I249, P293, F294

Table 1 (B): Molecular docking results of top ten Paritaprevir derivatives including interactive amino acids from SARS-CoV-2 MPP.

PubChem ID of Paritaprevir derivatives	***IUPAC Name***	***Binding Energy (kcal/mol)***	***Involved Amino Acids with Positions***
CID 131982844	(3S,9Z,12R,15S,17R)-N-cyclopropylsulfonyl-12-methyl-3-[(5-methylpyrazine-2-carbonyl)amino]-2,14-dioxo-17-phenanthridin-6-yloxy-1,13-diazabicyclo[13.3.0]octadec-9-ene-12-carboxamide	-16.3	H41, C145, H164, M165, E166, P168, D187, R188, Q189
CID 117860584	(1S,4R,6S,7Z,14S,18R)-N-cyclopropylsulfonyl-18-(3,9-difluorophenanthridin-6-yl)oxy-14-[(1-methylpyrazole-4-carbonyl)amino]-2,15-dioxo-3,16-diazatricyclo[14.3.0.04,6]nonadec-7-ene-4-carboxamide	-16.1	T25, T26, L27, H41, M49, F140, L141, N142, G143, C145, H164, M165, E166, D187, Q189
CID 144881776	(4S,6R,10S,16Z)-N-cyclopropylsulfonyl-10-[(5-methylpyrazine-2-carbonyl)amino]-3,9-dioxo-6-phenanthridin-6-yloxy-2,8-diazatricyclo[15.2.1.04,8]icos-16-ene-1-carboxamide	-16.1	T26, H41, M49, , F140, L141, N142, C145,H163, H164, M165, E166, R188, Q189
CID 144881777	(4S,6R,10S,16Z)-N-cyclopropylsulfonyl-10-[(5-methylpyrazine-2-carbonyl)amino]-3,9-dioxo-6-phenanthridin-6-yloxy-2,8-diazatricyclo[15.2.1.04,8]icos-16-ene-1-carboxamide	-16	H41, M49, , F140, L141, N142, C145,H163, H164, M165, E166, R188, Q189
CID 89997958	(1R,4S,6R,10S,16Z)-N-cyclopropylsulfonyl-10-[(5-methylpyrazine-2-carbonyl)amino]-3,9-dioxo-6-phenanthridin-6-yloxy-2,8-diazatricyclo[15.2.1.04,8]icos-16-ene-1-carboxamide	-15.5	T26, L27, H41, M49, Y54, , F140, L141, N142, G143, C145, H164, M165, E166, D187, Q189
CID 90479564	(1S,4R,6S,7Z,14S,18R)-N-cyclopropylsulfonyl-14-[(5-methylpyrazine-2-carbonyl)amino]-2,15-dioxo-18-phenanthridin-6-yloxy-3,16-diazatricyclo[14.3.0.04,6]nonadec-7-ene-4-carboxamide;dihydrate	-15.2	T25, H41, M49, F140, N142, C145, H163, H165, E166, P168, R188, Q189, T190
CID 117930281	(1S,4R,6S,7Z,14S)-N-cyclopropylsulfonyl-14-[(5-methylpyrazine-2-carbonyl)amino]-2,15-dioxo-18-phenanthridin-6-yloxy-3,16-diazatricyclo[14.3.0.04,6]nonadec-7-ene-4-carboxamide	-15.2	T25, L27, H41, M49, F140, N142, C145, M165, E166, P168, R188, Q189, T190
CID 126760198	(1S,4R,7Z,14S,18R)-N-cyclopropylsulfonyl-14-[(5-methylpyrazine-2-carbonyl)amino]-2,15-dioxo-18-phenanthridin-6-yloxy-3,16-diazatricyclo[14.3.0.04,6]nonadec-7-ene-4-carboxamide	-15.2	T25, L27, H41, M49, F140, N142, C145, M165, E166, P168, R188, Q189, T190
CID 130368695	(1S,6S,7Z,14S,18R)-N-cyclopropylsulfonyl-14-[(5-methylpyrazine-2-carbonyl)amino]-2,15-dioxo-18-phenanthridin-6-yloxy-3,16-diazatricyclo[14.3.0.04,6]nonadec-7-ene-4-carboxamide	-15.2	T25, H41, M49, F140, N142, C145, H163, M165, E166, P168, R188, Q189, T190
CID 129606829	(1R,4S,6R,7Z,14R,18S)-N-cyclopropylsulfonyl-14-[(5-methylpyrazine-2-carbonyl)amino]-2,15-dioxo-18-phenanthridin-6-yloxy-3,16-diazatricyclo[14.3.0.04,6]nonadec-7-ene-4-carboxamide	-15.2	T25, H41, M49, F140, N142, C145, H163, M165, E166, P168, R188, Q189, T190

Table 2: Molecular docking study of Hydroxychloroquine, Favipiravir, Remdesivir, alpha-ketoamide and MPP Inhibitors with MPPs of SARS-CoV-2 and HCV.

Ligand Candidates	***Main Protease Protein***	***Molecular Binding Energy (***kcal/mol***)***	***Involved Amino Acids with Positions***
alpha-ketoamide	SARS-CoV-2 (PDB ID: 6LU7)	-14.4	T25, L27, H41, M49, F140, N142, C145, H163, H164,pl M165, E166, H172,R188, Q189
HydroxyChloroquine	SARS-CoV-2 (PDB ID: 6LU7)	-5.0	T198, T199, Y236, Y239, L271, L272, L286, L287
Favipiravir	SARS-CoV-2 (PDB ID: 6LU7)	-4.7	L141, N142, G143, S144, C145, M165, E166
Remdesivir	SARS-CoV-2 (PDB ID: 6LU7)	-7.8	T25, T26, H41, M49, L141, N142, G143, C145, H164, M165, E166, D187, R188, Q189
Paritaprevir	SARS-CoV-2 (PDB ID: 6Y2E)	-10.9	K102, V104, Q107, Q110, N151, I152, D153, S158, T292, F294
Paritaprevir	HCV (PDB ID: 2P59)	-10.6	V26, K34, A1033, Q1035, R1037, L1039, C1042, S1063, R1135, H1136, S1159

Table 3: ADME analysis of top five MPP inhibitors by using SwissADME.

Parameter		***Topmost Main Protease Protein Inhibitors of SARS-CoV-2***				
		Paritaprevir	***Glecaprevir***	**Nelfinavir**	***Simeprevir***	***Lopinavir***
Physico-chemical parameters	Formula	C40H43N7O7S	C38H46F4N6O9S	C32H45N3O4S	C38H47N5O7S2	C37H48N4O5
	Molecular weight	765.88 g/mol	838.87 g/mol	567.78 g/mol	749.94 g/mol	628.80 g/mol
	Molar Refractivity	211.96	205.91	166.17	208.52	187.92
	TPSA	198.03 Å²	203.60 Å²	127.20 Å²	193.51 Å²	120.00 Å²
Lipophilicity	Log $P_{o/w}$ (iLOGP)	3.34	3.71	4.24	4.3	4.22
	Log $P_{o/w}$ (XLOGP3)	4.65	4.55	5.67	4.81	5.92
	Log $P_{o/w}$ (WLOGP)	3.89	5.69	4.37	5.51	3.57
	Log $P_{o/w}$ (MLOGP)	0.88	1.32	3.2	1.48	2.93
	Log $P_{o/w}$ (SILICOS-IT)	2.28	2.42	4.56	4.89	6.02
	Consensus Log $P_{o/w}$	3.01	3.54	4.41	4.2	4.53
Pharmaco-kinetics	GI absorption	Low	Low	Low	Low	High
	BBB permeant	No	No	No	No	No
	P-gp substrate	Yes	Yes	Yes	Yes	Yes
	CYP1A2 inhibitor	No	No	No	No	No
	CYP2C19 inhibitor	No	No	Yes	No	Yes
	CYP2C9 inhibitor	No	No	No	No	No
	CYP2D6 inhibitor	No	No	No	No	No
	CYP3A4 inhibitor	Yes	No	Yes	Yes	Yes
	Log K_p (skin permeation)	-7.67 cm/s	-8.19 cm/s	-5.74 cm/s	-7.46 cm/s	-5.93 cm/s
	Log *S* (SILICOS-IT)	-9.74	-7.96	-7.26	-8.79	-10.05
Water Solubility	Solubility	1.38e-07 mg/ml ; 1.81e-10 mol/l	9.22e-06 mg/ml ; 1.10e-08 mol/l	3.11e-05 mg/ml ; 5.48e-08 mol/l	1.21e-06 mg/ml ; 1.61e-09 mol/l	5.57e-08 mg/ml ; 8.85e-11 mol/l

Supplementary Tables

Supplementary Table 1: List of all approved Main Protease Protein (MPP) inhibitors retrieved from the DrugBank of NCBI

MPP inhibitors	***DrugBank ID***	***Group***	***Description***
Amprenavir	DB00701	Approved, Investigational	HIV protease inhibitor
Asunaprevir	DB11586	Approved, Investigational, Withdrawn	NS3 protease inhibitor
Atazanavir	DB01072	Approved, Investigational	antiretroviral protease inhibitor
Paritaprevir	DB09297	Approved, Investigational	HCV NS3/4A protease inhibitor
Grazoprevir	DB11575	Approved	HCV NS3/4A protease inhibitor
Glecaprevir	DB13879	Approved, Investigational	HCV NS3/4A protease inhibitor
Ritonavir	DB00503	Approved, Investigational	HIV protease inhibitor
Nelfinavir	DB00220	Approved	HIV-1 protease inhibitor
Lopinavir	DB01601	Approved	antiretroviral protease inhibitor
Simeprevir	DB06290	Approved	HCV NS3/4A protease inhibitor
Telaprevir	DB05521	Approved, Withdrawn	HCV NS3/4A protease inhibitor
Indinavir	DB00224	Approved	specific HIV protease inhibitor
Darunavir	DB01264	Approved	HIV protease inhibitor
Fosamprenavir	DB01319	Approved	HIV protease inhibitor
Saquinavir	DB01232	Approved, Investigational	HIV protease inhibitor
Boceprevir	DB08873	Approved, Withdrawn	HCV NS3/4A protease inhibitor

Supplementary Table 2: List of the derivatives of Paritaprevir retrieved from NCBI.

PubChem ID	***IUPAC Name***
CID 131982844	(3S,9Z,12R,15S,17R)-N-cyclopropylsulfonyl-12-methyl-3-[(5-methylpyrazine-2-carbonyl)amino]-2,14-dioxo-17-phenanthridin-6-yloxy-1,13-diazabicyclo[13.3.0]octadec-9-ene-12-carboxamide
CID 117860584	(1S,4R,6S,7Z,14S,18R)-N-cyclopropylsulfonyl-18-(3,9-difluorophenanthridin-6-yl)oxy-14-[(1-methylpyrazole-4-carbonyl)amino]-2,15-dioxo-3,16-diazatricyclo[14.3.0.04,6]nonadec-7-ene-4-carboxamide
CID 144881776	(4S,6R,10S,16Z)-N-cyclopropylsulfonyl-10-[(5-methylpyrazine-2-carbonyl)amino]-3,9-dioxo-6-phenanthridin-6-yloxy-2,8-diazatricyclo[15.2.1.04,8]icos-16-ene-1-carboxamide
CID 144881777	(4S,6R,10S,16Z)-N-cyclopropylsulfonyl-10-[(5-methylpyrazine-2-carbonyl)amino]-3,9-dioxo-6-phenanthridin-6-yloxy-2,8-diazatricyclo[15.2.1.04,8]icos-16-ene-1-carboxamide
CID 89997958	(1R,4S,6R,10S,16Z)-N-cyclopropylsulfonyl-10-[(5-methylpyrazine-2-carbonyl)amino]-3,9-dioxo-6-phenanthridin-6-yloxy-2,8-diazatricyclo[15.2.1.04,8]icos-16-ene-1-carboxamide
CID 90479564	(1S,4R,6S,7Z,14S,18R)-N-cyclopropylsulfonyl-14-[(5-methylpyrazine-2-carbonyl)amino]-2,15-dioxo-18-phenanthridin-6-yloxy-3,16-diazatricyclo[14.3.0.04,6]nonadec-7-ene-4-carboxamide;dihydrate
CID 117930281	(1S,4R,6S,7Z,14S)-N-cyclopropylsulfonyl-14-[(5-methylpyrazine-2-carbonyl)amino]-2,15-dioxo-18-phenanthridin-6-yloxy-3,16-diazatricyclo[14.3.0.04,6]nonadec-7-ene-4-carboxamide
CID 126760198	(1S,4R,7Z,14S,18R)-N-cyclopropylsulfonyl-14-[(5-methylpyrazine-2-carbonyl)amino]-2,15-dioxo-18-phenanthridin-6-yloxy-3,16-diazatricyclo[14.3.0.04,6]nonadec-7-ene-4-carboxamide
CID 130368695	(1S,6S,7Z,14S,18R)-N-cyclopropylsulfonyl-14-[(5-methylpyrazine-2-carbonyl)amino]-2,15-dioxo-18-phenanthridin-6-yloxy-3,16-diazatricyclo[14.3.0.04,6]nonadec-7-ene-4-carboxamide

CID 129606829	(1R,4S,6R,7Z,14R,18S)-N-cyclopropylsulfonyl-14-[(5-methylpyrazine-2-carbonyl)amino]-2,15-dioxo-18-phenanthridin-6-yloxy-3,16-diazatricyclo[14.3.0.04,6]nonadec-7-ene-4-carboxamide
CID 134503655	(1S,4R,7Z,14S)-N-cyclopropylsulfonyl-14-[(5-methylpyrazine-2-carbonyl)amino]-2,15-dioxo-18-phenanthridin-6-yloxy-3,16-diazatricyclo[14.3.0.04,6]nonadec-7-ene-4-carboxamide
CID 91971755	(1S,4R,6S,7Z,14S,18R)-14-[(5-methylpyrazine-2-carbonyl)amino]-2,15-dioxo-18-phenanthridin-6-yloxy-N-(2,2,3,3-tetradeuteriocyclopropyl)sulfonyl-3,16-diazatricyclo[14.3.0.04,6]nonadec-7-ene-4-carboxamide
CID 129190351	(1*S*,4*R*,7*Z*,18*R*)-*N*-cyclopropylsulfonyl-14-[(5-methylpyrazine-2-carbonyl)amino]-2,15-dioxo-18-phenanthridin-6-yloxy-3,16-diazatricyclo[14.3.0.0^{4,6}]nonadec-7-ene-4-carboxamide
CID 134689630	(7*Z*)-*N*-cyclopropylsulfonyl-14-[(5-methylpyrazine-2-carbonyl)amino]-2,15-dioxo-18-phenanthridin-6-yloxy-3,16-diazatricyclo[14.3.0.0^{4,6}]nonadec-7-ene-4-carboxamide
CID 76528926	*N*-cyclopropylsulfonyl-8,8-difluoro-14-[(5-methylpyrazine-2-carbonyl)amino]-2,15-dioxo-18-phenanthridin-6-yloxy-3,16-diazatricyclo[14.3.0.0^{4,6}]nonadecane-4-carboxamide
CID 57415626	(1*S*,4*R*,6*S*,14*S*,18*R*)-*N*-cyclopropylsulfonyl-8,8-difluoro-14-[(5-methylpyrazine-2-carbonyl)amino]-2,15-dioxo-18-phenanthridin-6-yloxy-3,16-diazatricyclo[14.3.0.0^{4,6}]nonadecane-4-carboxamide
CID 132247343	(3*S*,9*Z*,12*R*,15*S*,17*R*)-*N*-cyclopropylsulfonyl-11-methyl-3-[(5-methylpyrazine-2-carbonyl)amino]-2,14-dioxo-17-phenanthridin-6-yloxy-1,13-diazabicyclo[13.3.0]octadec-9-ene-12-carboxamide
CID 123539122	*N*-cyclopropylsulfonyl-9,9-difluoro-12-methyl-3-[(5-methylpyrazine-2-carbonyl)amino]-2,14-dioxo-17-phenanthridin-6-yloxy-1,13-diazabicyclo[13.3.0]octadecane-12-carboxamide
CID 68500653	(1*S*,4*R*,6*S*,14*S*,18*R*)-*N*-cyclopropylsulfonyl-14-[(5-methylpyrazine-2-carbonyl)amino]-2,15-dioxo-18-phenanthridin-6-yloxy-3,16-diazatricyclo[14.3.0.0^{4,6}]nonadec-7-ene-4-carboxamide

CID 139266795	*N*-cyclopropylsulfonyl-14-[(5-methylpyrazine-2-carbonyl)amino]-2,15-dioxo-18-phenanthridin-6-yloxy-3,16-diazatricyclo[14.3.0.0^{4,6}]nonadec-7-ene-4-carboxamide;dihydrate
CID 140642412	(7*Z*)-*N*-cyclopropylsulfonyl-2,15-dioxo-18-phenanthridin-6-yloxy-14-(pyrazine-2-carbonylamino)-3,16-diazatricyclo[14.3.0.0^{4,6}]nonadec-7-ene-4-carboxamide
CID 75093025	*N*-cyclopropylsulfonyl-14-[(5-methylpyrazine-2-carbonyl)amino]-2,15-dioxo-18-phenanthridin-6-yloxy-3,16-diazatricyclo[14.3.0.0^{4,6}]nonadec-7-ene-4-carboxamide
CID 123207199	*N*-cyclopropylsulfonyl-14-[(5-methylpyrazine-2-carbonyl)amino]-2-oxo-18-phenanthridin-6-yloxy-3,16-diazatricyclo[14.3.0.0^{4,6}]nonadec-7-ene-4-carboxamide
CID 45110641	(1*S*,4*R*,6*S*,7*Z*,14*S*,18*R*)-*N*-cyclopropylsulfonyl-2,15-dioxo-18-phenanthridin-6-yloxy-14-(pyridazine-4-carbonylamino)-3,16-diazatricyclo[14.3.0.0^{4,6}]nonadec-7-ene-4-carboxamide
CID 126970090	(1*R*,4*R*,6*S*,14*S*,18*R*)-*N*-cyclopropylsulfonyl-14-[(5-methylpyrazine-2-carbonyl)amino]-2,15-dioxo-18-phenanthridin-6-yloxy-3,16-diazatricyclo[14.3.0.0^{4,6}]nonadec-7-ene-4-carboxamide
CID 134693118	(1*S*,4*R*)-*N*-cyclopropylsulfonyl-14-[(5-methylpyrazine-2-carbonyl)amino]-2,15-dioxo-18-phenanthridin-6-yloxy-3,16-diazatricyclo[14.3.0.0^{4,6}]nonadec-7-ene-4-carboxamide
CID 145142292	(1*S*,4*R*,8*Z*,15*S*,19*R*)-*N*-cyclopropylsulfonyl-15-[(5-methylpyrazine-2-carbonyl)amino]-2,16-dioxo-19-phenanthridin-6-yloxy-3,17-diazatricyclo[15.3.0.0^{4,7}]icosa-5,8-diene-4-carboxamide
CID 134322927	(3*S*,9*Z*,12*R*,15*S*,17*R*)-*N*-cyclopropylsulfonyl-11,12-dimethyl-3-[(5-methylpyrazine-2-carbonyl)amino]-2,14-dioxo-17-(phenanthridin-6-yloxymethyl)-1,13-diazabicyclo[13.3.0]octadec-9-ene-12-carboxamide
CID 67985746	(1*S*,4*R*,7*Z*,18*R*)-*N*-cyclopropylsulfonyl-2,15-dioxo-18-phenanthridin-6-yloxy-14-(pyrazine-2-carbonylamino)-3,16-diazatricyclo[14.3.0.0^{4,6}]nonadec-7-ene-4-carboxamide

CID 68496388	(1*S*,4*R*,6*S*,14*S*,18*R*)-*N*-cyclopropylsulfonyl-2,15-dioxo-18-phenanthridin-6-yloxy-14-(pyridazine-4-carbonylamino)-3,16-diazatricyclo[14.3.0.$0^{4,6}$]nonadec-7-ene-4-carboxamide
CID 45110639	(1*S*,4*R*,6*S*,7*Z*,14*S*,18*R*)-*N*-cyclopropylsulfonyl-2,15-dioxo-18-phenanthridin-6-yloxy-14-(pyrazine-2-carbonylamino)-3,16-diazatricyclo[14.3.0.$0^{4,6}$]nonadec-7-ene-4-carboxamide
CID 144678769	(1*S*,4*S*,7*Z*,14*S*,18*R*)-*N*-cyclopropylsulfonyl-5-methylidene-14-[(5-methylpyrazine-2-carbonyl)amino]-2,15-dioxo-18-(phenanthridin-6-yloxymethyl)-3,16-diazatricyclo[14.3.0.$0^{4,6}$]nonadec-7-ene-4-carboxamide
CID 68498031	(1*S*,4*R*,6*R*,7*Z*,14*S*,18*R*)-*N*-cyclopropylsulfonyl-14-[(5-methylpyrazine-2-carbonyl)amino]-2,15-dioxo-18-phenanthridin-6-yloxy-3,16-diazatricyclo[14.3.0.$0^{4,6}$]nonadec-7-ene-4-carboxamide
CID 132207185	(1*S*,4*R*,7*Z*,14*S*,18*R*)-*N*-cyclopropylsulfonyl-14-[(5-methylpyrazine-2-carbonyl)amino]-2,15-dioxo-18-(phenanthridin-6-yloxymethyl)-3,16-diazatricyclo[14.3.0.$0^{4,6}$]nonadec-7-ene-4-carboxamide
CID 123457581	*N*-cyclopropylsulfonyl-8,8-difluoro-5-methyl-14-[(5-methylpyrazine-2-carbonyl)amino]-2,15-dioxo-18-phenanthridin-6-yloxy-3,16-diazatricyclo[14.3.0.$0^{4,6}$]nonadecane-4-carboxamide
CID 68494543	*N*-ethylethanamine;(1*S*,4*R*,6*S*,7*Z*,14*S*,18*R*)-14-[(5-methylpyrazine-2-carbonyl)amino]-2,15-dioxo-18-phenanthridin-6-yloxy-3,16-diazatricyclo[14.3.0.$0^{4,6}$]nonadec-7-ene-4-carboxylic acid
CID 68494548	(1*S*,4*R*,6*S*,14*S*,18*R*)-14-[(5-methylpyrazine-2-carbonyl)amino]-2,15-dioxo-18-phenanthridin-6-yloxy-3,16-diazatricyclo[14.3.0.$0^{4,6}$]nonadec-7-ene-4-carboxylic acid
CID 140642415	(7*Z*)-*N*-cyclopropylsulfonyl-2,15-dioxo-18-phenanthridin-6-yloxy-14-(pyridazine-4-carbonylamino)-3,16-diazatricyclo[14.3.0.$0^{4,6}$]nonadec-7-ene-4-carboxamide
CID 144411760	(1*S*,4*S*,15*S*,19*R*)-*N*-cyclopropylsulfonyl-9,9-difluoro-15-[(5-methylpyrazine-2-carbonyl)amino]-2,16-dioxo-19-phenanthridin-6-yloxy-3,17-diazatricyclo[15.3.0.$0^{4,7}$]icos-5-yne-4-carboxamide

CID 144411796	(1*S*,4*R*,14*S*,18*R*)-*N*-cyclopropylsulfonyl-8,8-difluoro-5-methyl-14-[(5-methylpyrazine-2-carbonyl)amino]-2,15-dioxo-18-phenanthridin-6-yloxy-3,16-diazatricyclo[14.3.0.$0^{4,6}$]nonadecane-4-carboxamide
CID 123172379	*N*-cyclopropylsulfonyl-12-methyl-3-[(5-methylpyrazine-2-carbonyl)amino]-2,14-dioxo-17-phenanthridin-6-yloxy-1,13-diazabicyclo[13.3.0]octadec-9-ene-12-carboxamide
CID 58001490	*N*-[(2*S*)-1-[(2*S*)-2-[[(1*R*,2*S*)-1-(cyclopropylsulfonylcarbamoyl)-2-ethenylcyclopropyl]carbamoyl]-4-(7-methoxy-2-phenylquinolin-4-yl)oxypyrrolidin-1-yl]-3-[methyl(prop-2-enoyl)amino]-1-oxopropan-2-yl]pyrazine-2-carboxamide
CID 123747270	*N*-cyclopropylsulfonyl-6-methylidene-15-[(5-methylpyrazine-2-carbonyl)amino]-2,16-dioxo-19-phenanthridin-6-yloxy-3,17-diazatricyclo[15.3.0.$0^{4,7}$]icos-8-ene-4-carboxamide
CID 139598190	(1*S*,4*R*,14*S*,18*R*)-14-[(5-methylpyrazine-2-carbonyl)amino]-2,15-dioxo-18-phenanthridin-6-yloxy-3,16-diazatricyclo[14.3.0.$0^{4,6}$]nonadec-7-ene-4-carboxylic acid
CID 77506125	3-*O*-*tert*-butyl 4-*O*-ethyl 14-[(5-methylpyrazine-2-carbonyl)amino]-2,15-dioxo-18-phenanthridin-6-yloxy-3,16-diazatricyclo[14.3.0.$0^{4,6}$]nonadec-7-ene-3,4-dicarboxylate
CID 87473268	(1*S*,4*R*,6*R*,7*E*,14*S*,18*R*)-*N*-cyclopropylsulfonyl-14-[(5-methylpyrazine-2-carbonyl)amino]-2,15-dioxo-18-phenanthridin-6-yloxy-3,16-diazatricyclo[14.3.0.$0^{4,6}$]nonadec-7-ene-4-carboxamide
CID 133548468	(1*R*,4*S*,6*R*,7*E*,14*R*,18*S*)-*N*-cyclopropylsulfonyl-14-[(5-methylpyrazine-2-carbonyl)amino]-2,15-dioxo-18-phenanthridin-6-yloxy-3,16-diazatricyclo[14.3.0.$0^{4,6}$]nonadec-7-ene-4-carboxamide
CID 123942813	ethyl (1*S*,4*R*,6*S*,14*S*,18*R*)-14-[(5-methylpyrazine-2-carbonyl)amino]-2,15-dioxo-18-phenanthridin-6-yloxy-3,16-diazatricyclo[14.3.0.$0^{4,6}$]nonadec-7-ene-4-carboxylate
CID 68499876	(1*S*,4*R*,6*S*,7*Z*,14*S*,18*R*)-14-amino-*N*-cyclopropylsulfonyl-2,15-dioxo-18-phenanthridin-6-yloxy-3,16-diazatricyclo[14.3.0.$0^{4,6}$]nonadec-7-ene-4-carboxamide

CID 143897349	(1*S*,4*R*,6*R*,14*S*,18*R*)-14-anilino-*N*-cyclopropylsulfonyl-18-isoquinolin-1-yloxy-2,15-dioxo-3,16-diazatricyclo[14.3.0.0^{4,6}]nonadecane-4-carboxamide
CID 87474442	(1*S*,4*R*,6*S*,7*E*,14*S*,18*R*)-14-amino-*N*-cyclopropylsulfonyl-2,15-dioxo-18-phenanthridin-6-yloxy-3,16-diazatricyclo[14.3.0.0^{4,6}]nonadec-7-ene-4-carboxamide
CID 123706840	*N*-cyclopropylsulfonyl-5-methylidene-14-[(5-methylpyrazine-2-carbonyl)amino]-2,15-dioxo-18-phenanthridin-6-yloxy-3,16-diazatricyclo[14.3.0.0^{4,6}]nonadec-7-ene-4-carboxamide
CID 123764424	*N*-cyclopropylsulfonyl-15-[(5-methylpyrazine-2-carbonyl)amino]-2,16-dioxo-19-phenanthridin-6-yloxy-3,17-diazatricyclo[15.3.0.0^{4,7}]icos-8-ene-4-carboxamide
CID 144881773	*N*-[(1*S*,4*R*,7*Z*,14*S*,18*R*)-18-(7,8-dihydrophenanthridin-6-yloxy)-2,15-dioxo-3,16-diazatricyclo[14.3.0.0^{4,6}]nonadec-7-en-14-yl]-5-methylpyrazine-2-carboxamide
CID 44180178	*N*-[(2*S*)-1-[(2*S*,4*R*)-2-[[(1*R*,2*S*)-1-(cyclopropylsulfonylcarbamoyl)-2-ethenylcyclopropyl]carbamoyl]-4-(7-methoxy-2-phenylquinolin-4-yl)oxypyrrolidin-1-yl]-3-[methyl(prop-2-enoyl)amino]-1-oxopropan-2-yl]pyrazine-2-carboxamide
CID 131982843	(1*S*,4*R*,8*Z*,15*S*,19*R*)-*N*-cyclopropylsulfonyl-15-[(5-methylpyrazine-2-carbonyl)amino]-2,16-dioxo-19-phenanthridin-6-yloxy-3,17-diazatricyclo[15.3.0.0^{4,7}]icos-8-ene-4-carboxamide
CID 73211765	(1*S*,4*R*,6*S*,7*Z*,14*S*,18*R*)-*N*-cyclopropylsulfonyl-14-[(5-methylpyrazine-2-carbonyl)amino]-2,15-dioxo-18-phenanthridin-6-yloxy-3,16-diazatricyclo[14.3.0.0^{4,6}]nonadec-7-ene-4-carboxamide;hydrate
CID 89997539	(1*S*,4*R*,6*S*,7*Z*,18*R*)-1-[6-(cyclopropylsulfonylcarbamoyl)-3-methylpyrazin-2-yl]-2,15-dioxo-18-phenanthridin-6-yloxy-3,16-diazatricyclo[14.3.0.0^{4,6}]nonadec-7-ene-4-carboxamide
CID 123658396	*N*-cyclopropylsulfonyl-12-ethyl-3-[(5-methylpyrazine-2-carbonyl)amino]-2,14-dioxo-17-phenanthridin-6-yloxy-1,13-diazabicyclo[13.3.0]octadec-9-ene-12-carboxamide

CID 16075882	*tert*-butyl *N*-[(2*S*)-1-[(2*S*,4*R*)-2-[[(1*R*,2*S*)-1-(cyclopropylsulfonylcarbamoyl)-2-ethenylcyclopropyl]carbamoyl]-4-(3-pyrazin-2-ylisoquinolin-1-yl)oxypyrrolidin-1-yl]-3,3-dimethyl-1-oxobutan-2-yl]carbamate
CID 23595603	*tert*-butyl *N*-[1-[2-[[1-(cyclopropylsulfonylcarbamoyl)-2-ethenylcyclopropyl]carbamoyl]-4-(3-pyrazin-2-ylisoquinolin-1-yl)oxypyrrolidin-1-yl]-3,3-dimethyl-1-oxobutan-2-yl]carbamate
CID 123202053	*N*-[2-ethenyl-1-[(1-methylcyclopropyl)sulfonylcarbamoyl]cyclopropyl]-22,25-dioxo-11-pyridin-4-yl-2,21-dioxa-4,23,26-triazapentacyclo[24.2.1.$0^{3,12}$.$0^{5,10}$.$0^{18,20}$]nonacosa-3,5,7,9,11-pentaene-27-carboxamide
CID 87476180	(1*S*,4*R*,6*S*,7*E*,14*S*,18*R*)-*N*-cyclopropylsulfonyl-2,15-dioxo-18-phenanthridin-6-yloxy-14-(pyrazine-2-carbonylamino)-3,16-diazatricyclo[14.3.0.$0^{4,6}$]nonadec-7-ene-4-carboxamide
CID 87475090	(1*S*,4*R*,6*S*,7*E*,14*S*,18*R*)-*N*-cyclopropylsulfonyl-14-[(5-methylpyrazine-2-carbonyl)amino]-2,15-dioxo-18-phenanthridin-6-yloxy-3,16-diazatricyclo[14.3.0.$0^{4,6}$]nonadec-7-ene-4-carboxamide
CID 117625846	(1*R*,18*R*,20*R*,24*S*,27*S*)-24-cyclohexyl-*N*-[(3*S*)-3-ethyl-1-[(1-methylcyclopropyl)sulfonylamino]-1-oxopent-4-en-2-yl]-22,25-dioxo-11-pyridin-4-yl-2,21-dioxa-4,23,26-triazapentacyclo[24.2.1.$0^{3,12}$.$0^{5,10}$.$0^{18,20}$]nonacosa-3,5,7,9,11-pentaene-27-carboxamide
CID 87471819	*N*-ethylethanamine;(1*S*,4*R*,6*S*,7*E*,14*S*,18*R*)-14-[(5-methylpyrazine-2-carbonyl)amino]-2,15-dioxo-18-phenanthridin-6-yloxy-3,16-diazatricyclo[14.3.0.$0^{4,6}$]nonadec-7-ene-4-carboxylic acid
CID 87473750	3-*O*-*tert*-butyl 4-*O*-ethyl (1*S*,4*R*,6*S*,7*E*,14*S*,18*R*)-14-[(5-methylpyrazine-2-carbonyl)amino]-2,15-dioxo-18-phenanthridin-6-yloxy-3,16-diazatricyclo[14.3.0.$0^{4,6}$]nonadec-7-ene-3,4-dicarboxylate
CID 23595490	*N*-[1-[2-[[1-(cyclopropylsulfonylcarbamoyl)-2-ethenylcyclopropyl]carbamoyl]-4-(6-methoxyisoquinolin-1-yl)oxypyrrolidin-1-yl]-3,3-dimethyl-1-oxobutan-2-yl]pyrazine-2-carboxamide

CID 16075909	*N*-[(2*S*)-1-[(2*S*,4*R*)-2-[[(1*R*,2*S*)-1-(cyclopropylsulfonylcarbamoyl)-2-ethenylcyclopropyl]carbamoyl]-4-(6-methoxyisoquinolin-1-yl)oxypyrrolidin-1-yl]-3,3-dimethyl-1-oxobutan-2-yl]pyrazine-2-carboxamide
CID 58594019	*tert*-butyl (2*S*,4*R*)-2-[[(1*R*,2*S*)-1-(cyclopropylsulfonylcarbamoyl)-2-ethenylcyclopropyl]carbamoyl]-4-(3-pyridin-4-ylisoquinolin-1-yl)oxypyrrolidine-1-carboxylate
CID 68500752	(1*R*,2*S*)-2-ethenyl-2-ethyl-1-[(2-methylpropan-2-yl)oxycarbonyl-[(2*S*,4*R*)-1-[2-[(5-methylpyrazine-2-carbonyl)amino]non-8-enoyl]-4-phenanthridin-6-yloxypyrrolidine-2-carbonyl]amino]cyclopropane-1-carboxylic acid
CID 67296958	(1*R*,2*S*)-2-ethenyl-2-ethyl-1-[(2-methylpropan-2-yl)oxycarbonyl-[(2*S*,4*R*)-1-[(2*S*)-2-[(5-methylpyrazine-2-carbonyl)amino]non-8-enoyl]-4-phenanthridin-6-yloxypyrrolidine-2-carbonyl]amino]cyclopropane-1-carboxylic acid
CID 129900715	*N*-[2-[(1*S*,4*R*,6*S*,7*Z*,14*R*,18*R*)-4-(2-cyclopropylsulfonylacetyl)-2,15-dioxo-18-phenanthridin-6-yloxy-3,16-diazatricyclo[14.3.0.0^{4,6}]nonadec-7-en-14-yl]acetyl]-5-methylpyrazine-2-carboxamide
CID 23595731	*tert*-butyl 2-[[1-(cyclopropylsulfonylcarbamoyl)-2-ethenylcyclopropyl]carbamoyl]-4-(3-pyridin-4-ylisoquinolin-1-yl)oxypyrrolidine-1-carboxylate
CID 68498890	3-*O*-*tert*-butyl 4-*O*-ethyl (1*S*,4*R*,6*S*,7*Z*,14*S*,18*R*)-14-[(5-methylpyrazine-2-carbonyl)amino]-2,15-dioxo-18-phenanthridin-6-yloxy-3,16-diazatricyclo[14.3.0.0^{4,6}]nonadec-7-ene-3,4-dicarboxylate
CID 67983962	ethyl (1*S*,4*R*,6*S*,7*Z*,14*S*,18*R*)-14-[(5-methylpyrazine-2-carbonyl)amino]-2,15-dioxo-18-phenanthridin-6-yloxy-3,16-diazatricyclo[14.3.0.0^{4,6}]nonadec-7-ene-4-carboxylate
CID 87471820	(1*S*,4*R*,6*S*,7*E*,14*S*,18*R*)-14-[(5-methylpyrazine-2-carbonyl)amino]-2,15-dioxo-18-phenanthridin-6-yloxy-3,16-diazatricyclo[14.3.0.0^{4,6}]nonadec-7-ene-4-carboxylic acid
CID 58594100	*N*-[(2*S*)-1-[(2*S*)-2-[[(1*R*,2*S*)-1-(cyclopropylsulfonylcarbamoyl)-2-ethenylcyclopropyl]carbamoyl]-4-(6-methoxyisoquinolin-1-yl)oxypyrrolidin-1-yl]-3,3-dimethyl-1-oxobutan-2-yl]pyrazine-2-carboxamide

CID 87472503	(1*S*,4*R*,6*S*,7*E*,14*S*,18*R*)-*N*-cyclopropylsulfonyl-2,15-dioxo-18-phenanthridin-6-yloxy-14-(pyridazine-4-carbonylamino)-3,16-diazatricyclo[14.3.0.$0^{4,6}$]nonadec-7-ene-4-carboxamide
CID 68496037	ethyl (1*S*,4*R*,6*S*,7*Z*,14*S*,18*R*)-14-[(5-methylpyrazine-2-carbonyl)amino]-2,15-dioxo-18-phenanthridin-6-yloxy-3,16-diazatricyclo[14.3.0.$0^{4,6}$]nonadec-7-ene-4-carboxylate;hydrochloride
CID 87472307	(1*S*,4*R*,6*S*,7*E*,14*S*,18*R*)-19-ethyl-14-[(5-methylpyrazine-2-carbonyl)amino]-2,15-dioxo-18-phenanthridin-6-yloxy-3,16-diazatricyclo[14.3.0.$0^{4,6}$]nonadec-7-ene-4-carboxylic acid
CID 67296951	ethyl (1*R*,2*S*)-2-ethenyl-1-[(2-methylpropan-2-yl)oxycarbonyl-[(2*S*,4*R*)-1-[(2*S*)-2-[(5-methylpyrazine-2-carbonyl)amino]non-8-enoyl]-4-phenanthridin-6-yloxypyrrolidine-2-carbonyl]amino]cyclopropane-1-carboxylate
CID 141228784	ethyl (2*S*)-2-ethenyl-1-[(2-methylpropan-2-yl)oxycarbonyl-[(2*S*,4*R*)-1-[2-[(5-methylpyrazine-2-carbonyl)amino]non-8-enoyl]-4-phenanthridin-6-yloxypyrrolidine-2-carbonyl]amino]cyclopropane-1-carboxylate
CID 67296803	2-ethenyl-1-[[(2*S*)-2-[(5-methylpyrazine-2-carbonyl)amino]non-8-enoyl]-[(2*S*,4*R*)-4-phenanthridin-6-yloxypyrrolidine-2-carbonyl]amino]cyclopropane-1-carboxylic acid
CID 58594022	(2*S*,4*R*)-*N*-[(1*R*,2*S*)-1-(cyclopropylsulfonylcarbamoyl)-2-ethenylcyclopropyl]-4-(3-pyrazin-2-ylisoquinolin-1-yl)oxypyrrolidine-2-carboxamide
CID 58593964	*tert*-butyl (2*S*,4*R*)-2-[[(1*R*,2*S*)-1-(cyclopropylsulfonylcarbamoyl)-2-ethenylcyclopropyl]carbamoyl]-4-(3-pyrazin-2-ylisoquinolin-1-yl)oxypyrrolidine-1-carboxylate
CID 67296808	2-ethenyl-1-[[(2*S*,4*R*)-1-[(2*S*)-2-[(5-methylpyrazine-2-carbonyl)amino]non-8-enoyl]-4-phenanthridin-6-yloxypyrrolidine-2-carbonyl]amino]cyclopropane-1-carboxylic acid
CID 68494544	(1*S*,4*R*,6*S*,7*Z*,14*S*,18*R*)-14-[(5-methylpyrazine-2-carbonyl)amino]-2,15-dioxo-18-phenanthridin-6-yloxy-3,16-diazatricyclo[14.3.0.$0^{4,6}$]nonadec-7-ene-4-carboxylic acid

CID 68496262	2-ethenyl-1-[[(2*S*,4*R*)-1-[2-[(5-methylpyrazine-2-carbonyl)amino]non-8-enoyl]-4-phenanthridin-6-yloxypyrrolidine-2-carbonyl]amino]cyclopropane-1-carboxylic acid
CID 135001966	ethyl (1*R*,2*S*)-2-ethenyl-1-[[(2*S*,4*R*)-1-[(2*S*)-2-[(2-methylpropan-2-yl)oxycarbonyl-(5-methylpyrazine-2-carbonyl)amino]non-8-enoyl]-4-phenanthridin-6-yloxypyrrolidine-2-carbonyl]amino]cyclopropane-1-carboxylate
CID 23595521	*N*-[1-(cyclopropylsulfonylcarbamoyl)-2-ethenylcyclopropyl]-4-(3-pyrazin-2-ylisoquinolin-1-yl)oxypyrrolidine-2-carboxamide
CID 23595734	*tert*-butyl 2-[[1-(cyclopropylsulfonylcarbamoyl)-2-ethenylcyclopropyl]carbamoyl]-4-(3-pyrazin-2-ylisoquinolin-1-yl)oxypyrrolidine-1-carboxylate
CID 86660471	ethyl (1*R*,2*S*)-2-ethenyl-1-[[(2*S*,4*R*)-1-[(2*S*)-2-[(5-methylpyrazine-2-carbonyl)amino]non-8-enoyl]-4-phenanthridin-6-yloxypyrrolidine-2-carbonyl]amino]cyclopropane-1-carboxylate
CID 117804962	*N*-[(*Z*,2*S*)-1-[(2*S*,4*R*)-2-carbamoyl-4-phenanthridin-6-yloxypyrrolidin-1-yl]-9-[(1*S*,2*S*)-2-(cyclopropylsulfonylcarbamoyl)cyclopropyl]-1-oxonon-8-en-2-yl]-5-methylpyrazine-2-carboxamide
CID 144881772	*N*-cyclopropylsulfonylacetamide;*N*-[(1*S*,4*R*,7*Z*,14*S*,18*R*)-18-(7,8-dihydrophenanthridin-6-yloxy)-2,15-dioxo-3,16-diazatricyclo[14.3.0.0^{4,6}]nonadec-7-en-14-yl]-5-methylpyrazine-2-carboxamide
CID 68499875	(1*S*,4*R*,6*S*,7*Z*,14*S*,18*R*)-14-amino-*N*-cyclopropylsulfonyl-2,15-dioxo-18-phenanthridin-6-yloxy-3,16-diazatricyclo[14.3.0.0^{4,6}]nonadec-7-ene-4-carboxamide;hydrochloride
CID 87472306	(1*S*,4*R*,6*S*,7*E*,14*S*,18*R*)-19-ethyl-14-[(5-methylpyrazine-2-carbonyl)amino]-2,15-dioxo-18-phenanthridin-6-yloxy-3,16-diazatricyclo[14.3.0.0^{4,6}]nonadec-7-ene-4-carboxylic acid;hydrochloride
CID 87474441	(1*S*,4*R*,6*S*,7*E*,14*S*,18*R*)-14-amino-*N*-cyclopropylsulfonyl-2,15-dioxo-18-phenanthridin-6-yloxy-3,16-diazatricyclo[14.3.0.0^{4,6}]nonadec-7-ene-4-carboxamide;hydrochloride

Supplementary Table 3: Molecular Docking Result of Protease Inhibitors with Binding Energy.

Main Protease Protein Inhibitors	***Molecular Binding Affinity with SARS-C0V-2 (kcal/mol)***
Paritaprevir	-10.9
Glecaprevir	-9.3
Nelfinavir	-8.7
Simeprevir	-8.6
Lopinavir	-8.4
Ritonavir	-8.4
Telaprevir	-8.3
Grazoprevir	-8.3
Indinavir	-8.2
Amprenavir	-7.9
Atazanavir	-7.9
Darunavir	-7.9
Fosamprenavir	-7.9
Saquinavir	-7.9
Asunaprevir	-7.4
Boceprevir	-7.1

Supplementary Table 4: Molecular Docking Result of Paritaprevir derivatives.

Derivatives of Paritaprevir	*Molecular Binding Affinity with SARS-C0V-2 (kcal/mol)*	*Derivatives of Paritaprevir*	*Molecular Binding Affinity with SARS-C0V-2 (kcal/mol)*	*Derivatives of Paritaprevir*	*Molecular Binding Affinity with SARS-C0V-2 (kcal/mol)*
CID 131982844	-16.3	CID132207185	-14.4	CID117625846	-12.8
CID 117860584	-16.1	CID 123457581	-14.4	CID87471819	-12.7
CID 144881776	-16.1	CID68494543	-14.3	CID87473750	-12.7
CID 144881777	-16	CID68494548	-14.3	CID 23595490	-12.7
CID 89997958	-15.5	CID140642415	-14.3	CID16075909	-12.6
CID 90479564	-15.2	CID144411760	-14.3	CID58594019	-12.6
CID 117930281	-15.2	CID144411796	-14.3	CID68500752	-12.6
CID 126760198	-15.2	CID 123172379	-14.3	CID67296958	-12.5
CID 130368695	-15.2	CID58001490	-14.2	CID129900715	-12.5
CID 129606829	-15.2	CID123747270	-14.2	CID 23595731	-12.5
CID 134503655	-15.2	CID139598190	-14.2	CID68498890	-12.4
CID 91971755	-15.2	CID 77506125	-14.2	CID 67983962	-12.4
CID129190351	-15.1	CID87473268	-14.1	CID 87471820	-12.4
CID134689630	-15.1	CID133548468	-14.1	CID68499875	-12.1
CID 76528926	-15.1	CID123942813	-14	CID58594100	-12
CID57415626	-14.9	CID 68499876	-13.9	CID87472503	-12
CID132247343	-14.9	CID143897349	-13.8	CID68496037	-11.7
CID 123539122	-14.9	CID 87474442	-13.8	CID 87472307	-11.6
CID68500653	-14.8	CID123706840	-13.7	CID67296951	-11.5
CID139266795	-14.8	CID123764424	-13.7	CID141228784	-11.5
CID140642412	-14.8	CID144881773	-13.7	CID 67296803	-11.4
CID 75093025	-14.8	CID44180178	-13.6	CID58594022	-11.2
CID 123207199	-14.8	CID131982843	-13.6	CID58593964	-11.1
CID45110641	-14.7	CID 73211765	-13.5	CID67296808	-11.1
CID126970090	-14.7	CID 89997539	-13.5	CID 68494544	-11.1
CID134693118	-14.7	CID 123658396	-13.4	CID68496262	-11
CID145142292	-14.7	CID16075882	-13.3	CID135001966	-10.8
CID134322927	-14.7	CID 23595603	-13.3	CID 23595521	-10.8
CID 67985746	-14.7	CID 123202053	-13.2	CID 23595734	-10.4
CID 68496388	-14.7	CID87472306	-13.2	CID86660471	-10.1
CID45110639	-14.6	CID87476180	-13	CID 117804962	-8.7
CID144678769	-14.6	CID87474441	-12.9	CID144881772	-5.6
CID68498031	-14.4	CID87475090	-12.8		

Supplementary Table 5: ADME analysis of top ten Paritaprevir derivatives by using SwissADME.

Parameter		***PubChem ID of Paritaprevir derivatives***									
		CID 131982844	***CID 117860584***	***CID 144881776***	***CID 144881777***	***CID 89997958***	***CID 90479564***	***CID 117930281***	***CID 126760198***	***CID 130368695***	***CID 129606829***
Physico-chemical parameters	Formula	C40H45N7O7S	C39H41F2N7O7S	C41H45N7O7S	C41H45N7O7S	C39H41N7O7S	C40H47N7O9S	C40H43N7O7S	C40H43N7O7S	C40H43N7O7S	C40H43N7O7S
	Molecular weight	767.89 g/mol	789.85 g/mol	779.90 g/mol	779.90 g/mol	751.85 g/mol	801.91 g/mol	765.88 g/mol	765.88 g/mol	765.88 g/mol	765.88 g/mol
	Molar Refractivity	214.07	208.36	216.76	216.76	206.99	218.05	211.96	211.96	211.96	211.96
	TPSA	198.03 Å²	190.07 Å²	198.03 Å²	198.03 Å²	198.03 Å²	216.49 Å²	198.03 Å²	198.03 Å²	198.03 Å²	198.03 Å²
Lipophilicity	Log $P_{o/w}$ (iLOGP)	3.82	3.54	2.97	4.04	2.37	3.37	2.33	3.12	5.53	3.22
	Log $P_{o/w}$ (XLOGP3)	5.1	4.57	4.67	4.67	4.25	3.7	4.65	4.65	4.65	4.65
	Log $P_{o/w}$ (WLOGP)	4.28	4.65	4.43	4.43	3.58	3.76	3.89	3.89	3.89	3.89
	Log $P_{o/w}$ (MLOGP)	0.88	2.26	1.05	1.05	0.71	-0.59	0.88	0.88	0.88	0.88
	Log $P_{o/w}$ (SILICOS-IT)	2.59	2.18	2.91	2.91	1.74	2.28	2.28	2.28	2.28	2.28
	Consensus Log $P_{o/w}$	3.33	3.44	3.2	3.42	2.53	2.51	2.81	2.96	3.45	2.98
Pharmaco-kinetics Water	GI absorption	Low	Low	Low	Low	Low	Low	Low	Low	Low	Low
	BBB permeant	No	No	No	No	No	No	No	No	No	No
	P-gp substrate	Yes	Yes	Yes	Yes	Yes	Yes	Yes	Yes	Yes	Yes
	CYP1A2 inhibitor	No	No	No	No	No	No	No	No	No	No
	CYP2C19 inhibitor	No	No	No	No	No	No	No	No	No	No
	CYP2C9 inhibitor	No	No	No	No	Yes	No	No	No	No	No
	CYP2D6 inhibitor	No	No	No	No	No	No	No	No	No	No
	CYP3A4 inhibitor	Yes	No	Yes	Yes	Yes	Yes	Yes	Yes	Yes	Yes
	Log K_p (skin permeation)	-7.36 cm/s	-7.87 cm/s	-7.74 cm/s	-7.74 cm/s	-7.87 cm/s	-8.56 cm/s	-7.67 cm/s	-7.67 cm/s	-7.67 cm/s	-7.67 cm/s
	Log *S* (SILICOS-IT)	-10.09	-9.02	-10.45	-10.45	-9.38	-9.74	-9.74	-9.74	-9.74	-9.74
Water Solubility	Solubility	6.30e-08 mg/ml ; 8.20e-11 mol/l	7.53e-07 mg/ml ; 9.53e-10 mol/l	2.77e-08 mg/ml ; 3.56e-11 mol/l	2.77e-08 mg/ml ; 3.56e-11 mol/l	3.15e-07 mg/ml ; 4.19e-10 mol/l	1.45e-07 mg/ml ; 1.81e-10 mol/l	1.38e-07 mg/ml ; 1.81e-10 mol/l	1.38e-07 mg/ml ; 1.81e-10 mol/l	1.38e-07 mg/ml ; 1.81e-10 mol/l	1.38e-07 mg/ml ; 1.81e-10 mol/l